

Behavior of beams reinforced with different types of bars from glass fiber reinforced polymer (GFRP), Carbon fiber Reinforced Polymer (CFRP) and high tensile steel (HTS) Under Static Load.

Aly Abdel Zaher Elsayed¹, Mohamed Mahmoud Ahmed²,
And Haysam Salaheldin Mohammed Hassan^{3,*}

1, 2 Staff in Civil Engineering Department, Faculty of Engineering, Assiut University, Assiut, Egypt.

3 Civil Engineer, Assiut University, 2004.

Abstract: As it is known, fiber reinforced polymer (FRP) bars are typically quite different from those of steel bars and they depend mainly on both matrix and fibers type, as well as on their volume fraction; although generally, FRP bars have lower weight, lower modulus of elasticity, but higher strength than steel. In the other hand, FRP has disadvantages, for instance: no yielding before brittle rupture and low transverse strength.

In this research, we have investigated flexural behavior in reinforced concrete beams with bars from glass fiber-reinforced polymer (GFRP), bars from carbon fiber-reinforced polymer (CFRP) and bars from high tensile steel (HTS) under static load.

We have analyzed the different kinds of failure, ultimate moment capacity, deflection, load of first crack, how to create and expand cracks, tensile and compressive strains created on beam during loading for different ratios of bars and different type of concrete strength. In the first group will show the effect of the type of reinforcement with different ratio of reinforcement. In the second group will show the effect of the type of reinforcement with different concrete strength.

Results taken from the experimental tests have been compared with ACI 440 and they show that deflections, cracks pattern, mode of failure, strain diagrams, slip for all tested beams.

Keywords: high performance concrete, bars from glass fiber reinforced polymer (GFRP), bars from carbon fiber reinforced polymer (CFRP), bars from high tensile steel (HTS), static loading flexural behavior, ultimate moment, crack, deflection, strain, failure mode.

I. Introduction

From years ago, civil engineers have been searching alternatives to steels and alloys to combat the high costs of repair and maintenance of structures damaged by corrosion and heavy use. With progress made by the polymer industry in the world, researchers think that these materials should be used in building structures.

Following their researches, the thought of using polymer materials instead of steel in concrete structures, led to the entry of fiber reinforced polymer (FRP) into field structures and constructions. Fiber reinforced polymers (FRP) bars are non-corrosive and as such, they have higher strength than their steel counterparts. Also, they have been used in aggressive environments such as water treatment plants instead of steel (AlMusallam et al., 1997; Elsayed, 1998, 1997; Benmokrane et al., 1995, 1996; Brown and Bartholomew, 1993; Dietz et al., 1999; Duranovic et al., 1997; Grace et al., 1998; Masmoudi et al., 1998; Michaluk et al., 1998; Pecce et al., 2000; Thériault and Benmokrane, 1998).

The other merits of fiber reinforced polymer are derived from its light weight and non-magnetic characteristic (Thériault and Benmokrane, 1998; Yost et al., 2001; Tureyen and Frosch, 2002), but the use of these materials have been limited because of the low modulus of elasticity and low ductility of large creeps which these problems result to (Thériault and Benmokrane, 1998; Yost et al., 2001; Tureyen and Frosch, 2002; Yost et al., 2001). Also, the lack of ductility of the parts made, to include the lack of comprehensive codes and standards for these bars, are other disadvantages of these bars.

Researches done on concrete reinforced members with FRP show that, no yield stress was seen, bearing in mind the linear relation between stress and strain in FRP bars (Victor and Shuxin, 2002). Width and extent of cracks in these beams are further used in the steel specimens (Benmokrane et al., 1996; Vijay and GangaRao, 2001). Deflection of concrete beams with FRP also is very bigger than similar samples of RC beams with steel, around 4 times, and the diagram of their load-deflection is in a straight line (Saadatmanesh and Ehsani, 1991; Victor and Shuxin, 2002). In addition, the usage of high strength concrete is effective (Vijay and GangaRao, 2001; Yost and Gross, 2002). In some compressive rupture of these beams at ultimate loading, a descent of the neutral axis (N.A.) has been seen with an increase in loading (Vijay and GangaRao, 2001).

For the design of the flexural concrete reinforced members with FRP, various relations are presented with the basic assumptions of achieving these relations, and as such, they are used for the reinforced concrete

members with steel bars (ACI Committee 440, 2006; International Federation for Structural Concrete Task Group 9.3 (FRP reinforcement in RC structures) 2007 ; Faza and GangaRao, 1993), and the properties of FRP are used as a replacement of the steel properties. In these relations, a ratio of the balanced mode is defined and the ratio that is higher and smaller than the balanced mode will cause the rupture in the compressive area. Of course, in cases where the ratio of bars is smaller than the balanced mode and the rupture in the compressive zone, it indicates that the submitted relation of the ratio of bars in the balanced mode is not the exact criteria for determining the kind of failure.

Researches done in Assuit, university in EGYPT for Flexural Behavior of Concrete Beams Reinforced with Basalt Bars under Static and Repeated Loads; Abd Elkader. Ahmed.Haridy, 2014. And also, Shear Behavior of Concrete Beams Reinforced with Basalt Fiber Reinforced Polymer Rebar; Zakaria Hameed Awadallah Ibrahim, 2015.

II. Experimental Work

Fifteen reinforced beam were prepared with main reinforcement (GFRP) or (CFRP) or steel bars (H.T.S) having rectangular cross section equal to 12*30 cm. The considered span for all tested beams were 240cm as showed in fig (1). The study takes in to consideration the following parameters as show in table (1):

1. Type of the main reinforcement bars (GFRP, CFRP and steel bars H.T.S).
2. Type of the used concrete strength f_c (400,650 and 900 Kg/cm²).

These beams divided in five group each group have separate comparison case. Two group have 6 beams changing in concrete strength value $f_c = 400$ and 650 Kg/cm² by the same A_g & A_c & A_s

Three group have 9 beams changing in A_g & A_c & A_s by The same concrete mix (high performance concrete ($f_c = 900$ Kg/cm²)).

2.1 Tested beams

Group D

This group consisted of three beams simply supported $b = 12$ cm $t = 30$ cm
 $L = 300$ cm concrete compressive strength ($f_c = 400$ Kg/cm²)
 A_g & A_c & $A_s = 2\emptyset 12, A_s = 2\emptyset 10, st. \emptyset 8 @ 15$ cm

Group.E

This group consisted of three beams simply supported $b = 12$ cm $t = 30$ cm
 $L = 300$ cm concrete compressive strength ($f_c = 650$ Kg/cm²)
 A_g & A_c & $A_s = 2\emptyset 12, A_s = 2\emptyset 10, st. \emptyset 8 @ 15$ cm

Group A

This group consisted of three beams simply supported $b = 12$ cm $t = 30$ cm
 $L = 300$ cm concrete compressive strength ($f_c = 900$ Kg/cm²)
 A_g & A_c & $A_s = 2\emptyset 10, A_s = 2\emptyset 10, st. \emptyset 8 @ 20$ cm

Group B

This group consisted of three beams simply supported $b = 12$ cm $t = 30$ cm
 $L = 300$ cm concrete compressive strength ($f_c = 900$ Kg/cm²)
 A_g & A_c & $A_s = 2\emptyset 12, A_s = 2\emptyset 10, st. \emptyset 8 @ 20$ cm

Group C

This group consisted of three beams simply supported $b = 12$ cm $t = 30$ cm
 $L = 300$ cm concrete compressive strength ($f_c = 900$ Kg/cm²) $A_g = 2\emptyset 16$ & $A_c = 4\emptyset 12$ & $A_s = 2\emptyset 16, A_s = 2\emptyset 10, st. \emptyset 8 @ 20$ cm

Table (1): Detail of tested beams

Group	Beam No.	Reinforcement type	b (cm)	d (cm)	Ar (cm ²)	fc (Kg/cm ²)
Group D	Dg12	GFRP	12	30	2Ø13	400
	Dc12	CFRP	12	30	2Ø13	400
	Ds12	Steel	12	30	2Ø12	400
Group E	Eg12	GFRP	12	30	2Ø13	650
	Ec12	CFRP	12	30	2Ø13	650
	Es12	Steel	12	30	2Ø12	650
Group A	Ag10	GFRP	12	30	2Ø9	900
	Ac10	CFRP	12	30	2Ø9	900
	As10	Steel	12	30	2Ø10	900
Group B	Bg12	GFRP	12	30	2Ø13	900
	Bc12	CFRP	12	30	2Ø13	900
	Bs12	Steel	12	30	2Ø12	900
Group C	Cg16	GFRP	12	30	2Ø16	900
	Cc(12+12)	CFRP	12	30	4Ø13	900
	Cs16	Steel	12	30	2Ø16	900

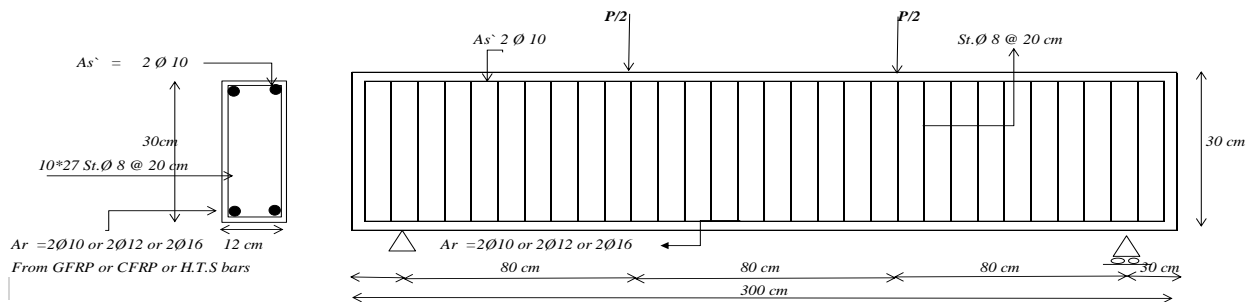


Fig. (1) Beam cross section and reinforcement

2.2 Materials

2.2.1 Concrete

Concrete mixes design was made to produce having cube compressive strengths of 400,650,900 kg/cm² after 28 days. The mix proportion by weight are presented in table (2), and table (2).

Table (2): Amount of constituent materials for the different mixes.

Mix No.	Amount of constituent materials /m ³ by weight						
	fc Kg/cm ²	Cement (kg.)	Sand (kg.)	Coarse aggr. (Kg.) Crushed basalt	Water (liter)	Silica fumes (kg.)	Add. (Kg.)
HPC1	400	450	591	1200	152	67.5	6.5
HPC2	650	500	496	1240	160	75	9.5
HPC3	900	500	550	1114	140	110	17.5

Table (3): Mix proportion for the different mixes:

Mix No.	1: n: m: w/c: S.F.: add.	fc (Kg/cm ²)
HPC1	1 : 1.31 : 2.65 : 0.35 : 15% : 1%	400
HPC2	1 : 0.99 : 2.48 : 0.32 : 15% : 1.9%	650
HPC3	1 : 1.10 : 2.23 : 0.28 : 22% : 3.5%	900

2.2.2 Reinforcement

2.2.2.1 GFRP Reinforcement

- 1- Glass Fibers are the most commonly used reinforcing fiber for polymeric matrix composites.
- 2- Molten glass can be drawn into continuous filament that is bundled into roving.
- 3- During fabrication, fiber surfaces are coated with a "sizing" to improve wetting by the matrix and provide better adhesion between the composite constituents.
- 4- Coating the glass fiber with a coupling agent provides a flexible layer at the inter face, improves the strength of the bond and reduce the number of voids in the material.
- 5- The most common glass fiber are made of E-glass, S-glass and Alkali-resistant glass.
- 6- E-glass is least expensive of all glass types and it has a wide application in fiber reinforced plastic industry.
- 7- S-glass has higher tensile strength, higher modulus and higher cost than E-glass.
- 8- Alkali-resistant (AR) glass fibers which help prevent corrosion by alkali attack in cement matrices are produced by adding zirconium.
- 9- AR-glass fibers with fiber sizing that are compatible with commonly utilized thermo set resins, however, are not currently available.
- 10- The tensile strength of glass fiber reduced at elevated temperatures but can be considered constant for the range of temperatures at which polymer matrices can be exposed.
- 11- The tensile strength also reduced with chemical corrosion and with under sustained loads.

2.2.2.2 CFRP Reinforcement

- 1- Carbon and graphite fibers are used interchangeably, but there are some significant differences between these two as far as their modular structure is concerned.
- 2- Most of the carbon fibers are produced by thermal decomposition of polyacrylonitrile (PAN).
- 3- The Carbon atoms are arranged in crystallographic parallel planes of regular hexagons to form graphite, while in carbon, the bonding between layers is weak, so that it has a two-dimensional ordering.
- 4- The manufacturing process for this type of fiber consists of oxidation at (200-300 C), different stages of carbonization at (1000-1500 C and 1500-2000 C) and finally graphitization at (2500-3000 C).
- 5- Graphite has a higher tensile modulus than carbon, therefore high-modulus fiber are produced by graphitization.
- 6- Carbon fibers are commercially available in long and continuous tows, which are bundles of 1,000 to 160,000 parallel filaments.
- 7- Carbon fibers exhibit high specific strength and stiffness; in general; as the elastic modulus increases ultimate tensile strength and failure elongation decrease
- 8- The tensile modulus and strength of carbon fibers are stable as temperature rises and also Carbon fiber has highly resistant to aggressive environmental factors.
- 9- The Carbon Fibers behave elastically to failure and fail in a brittle manner.
- 10- The most important disadvantage of carbon fibers is their high cost. Their cost is 10 to 30 times more expensive than E-glass .The cause of this high cost is the raw materials and the long process of carbonization and graphitization.

The Surface deformation patterns for commercially available GFRP and CFRP bars were shown in Fig. (2).

Manufacturing Steps of FRP is shown in, Fig. (3)

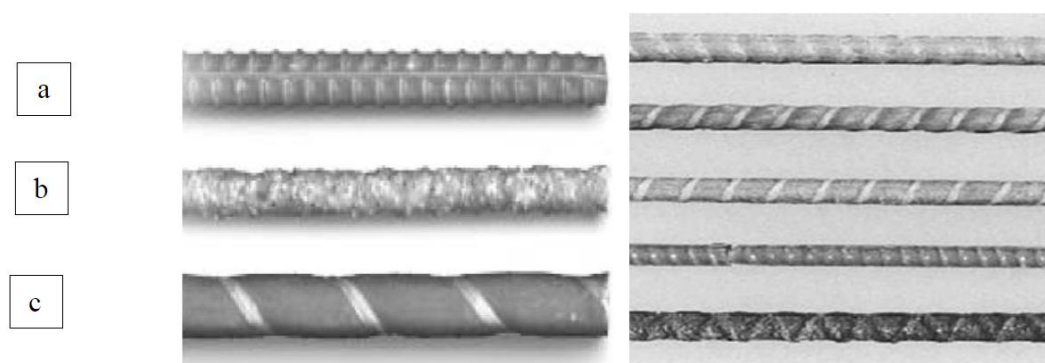


Fig. (2) Surface deformation patterns for commercially available FRP bars (a) ribbed & (b) sand- coated & (c) wrapped and sand coated.



Fig. (3) Manufacturing Steps of FRP.

The mechanical properties of the used reinforcement are given in tables (4) & (5)

Table (4) ASTM standard reinforcing bars for GFRP bars and CFRP bars.

Bar size designation		Nominal diameter, in. (mm)	Area, in. ² (mm ²)
Standard	Metric conversion		
No.3	No. 10	0.375 (9.5)	0.11 (71)
No.4	No. 13	0.500 (12.7)	0.20 (129)
No.5	No. 16	0.625 (15.9)	0.31 (199)

Table (5) Mechanical properties of the used GFRP bars and CFRP bars.

FRP Type	Bar Size Standard	Bar Size Metric conversion	Tensile Strength (MPa)	Ultimate Strain (%)	Modulus of Elasticity (GPa)
GFRP	No.3	No. 10	838.4	1.99	44.9
	No.4	No. 13	716	1.80	44.3
	No.5	No. 16	751.8	1.62	48.9
CFRP	No.3	No. 10	2136.9	1.92	131.8
	No.4	No. 13	2078.9	1.69	138.0

2.2.2.3 Steel Reinforcement

Deformed bars of high tensile steel were used as tension and compression reinforcement, as well as plain bars of normal mild steel were used for strips. The mechanical properties of the used steel reinforcement are given in table (6)

Table (6): Mechanical properties of the used steel

Commercial diameter(mm)	6	8	12	18	22
Actual diameter (mm)	5.85	8.1	12.2	17.9	22
Yield stress (kg/cm ²)	2419	2435	3626	3692	3711
Ultimate stress (kg/cm ²)	3620	3980	5878	6211	6352
% of elongation	26	26	30	28	27

2.3 Fabrication of the Tested Beams

The concrete was mixed mechanically and cast in steel forms. Control specimens including cube of 15 cm side length were cast from each mix. The beams and control specimens were sprayed with fresh water two times daily until the day before testing; all beams were tested at age of 28 days. Complete details of the tested beams are given in Table (1)

2.4 Test procedure

All beams were tested under two point static loading at ages of 28 days; each of the tested beams was loaded by a minimum load with increment of 0.5 tons; this minimum load was kept constant between two successive increments for about five minutes. During this period, readings of the electrical strain gauges for concrete and steel strain, dial gauges for deflection, and the cracks propagation were recorded at the beginning and at the end of each increment of loading up to failure.

2.5 Measured strains of concrete and steel

Strains of concrete and steel were measured by means of electrical strain gauges at the shown positions in Fig (4). The gauge length was 52mm, and the 800mm resistance was 600 ohms and gauge factor $(2 \pm 0.75\%)$. Strain gauges were connected to strain indicator with its box resistance. The deflection was measured by dial gauge with accuracy of 0.01mm fixed at the position of maximum deflection for each beam as shown in fig (4).

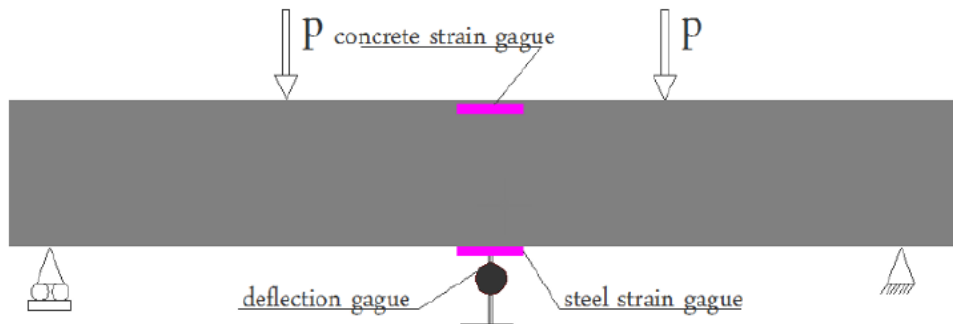


Fig. (4) Method of measuring deformation of beams

III. Test Result

3.1 Crack pattern and mode of failure

The cracks pattern and modes of failure are explained for the tested concrete beams under the static loading. Fifteen rectangular beams have same dimension 12.5 cm * 30 cm and 2.4m span with the same outer free cant liver 30 cm from each side outer the support to achieve beam length 3m. The beams divided to five groups due to difference in the type of the reinforcement and their compressive strength as mention in table (1) the cracking and ultimate loads were summarized at table (7) and mode of failure was as follow:

Group D

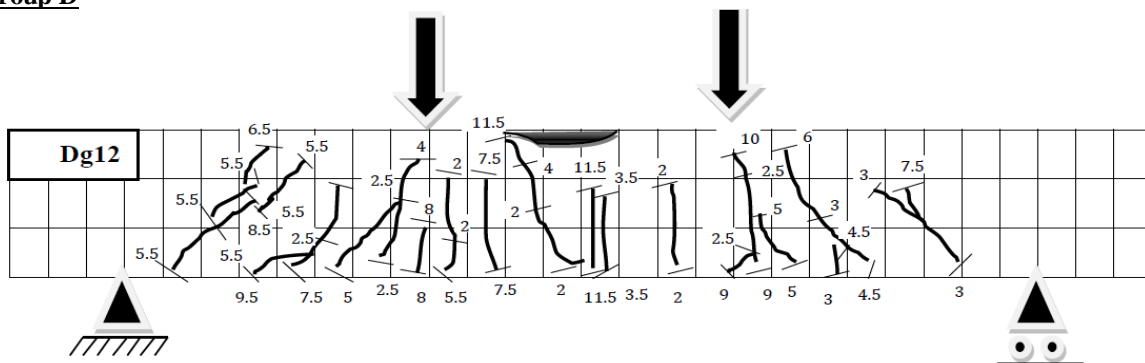


Fig. (5): Crack pattern of beam (Dg12)



Fig. (6): Shape of failure of beam (Dg12)

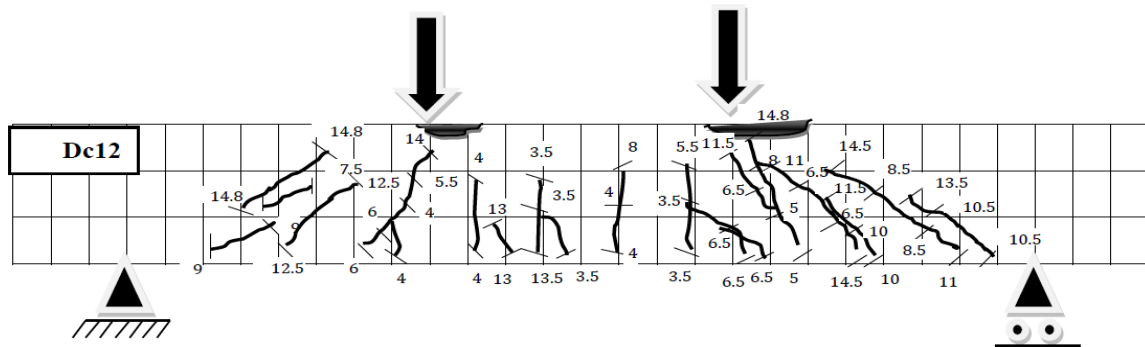


Fig. (7): Crack pattern of beam (Dc12)

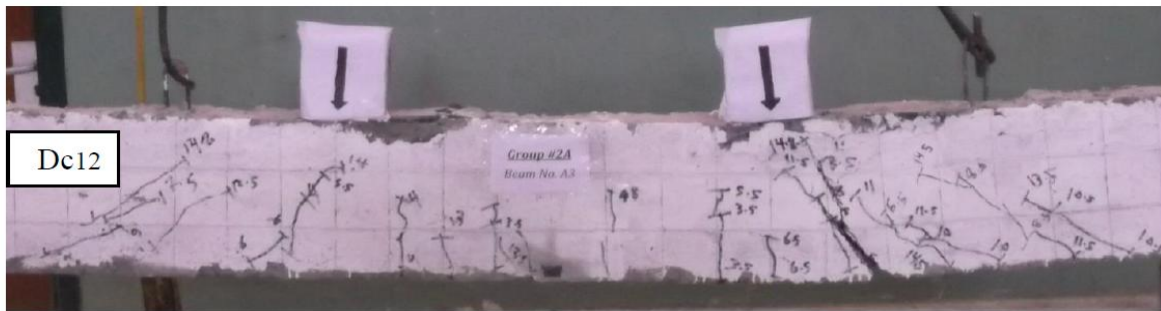


Fig. (8): Shape of failure of beam (Dc12)

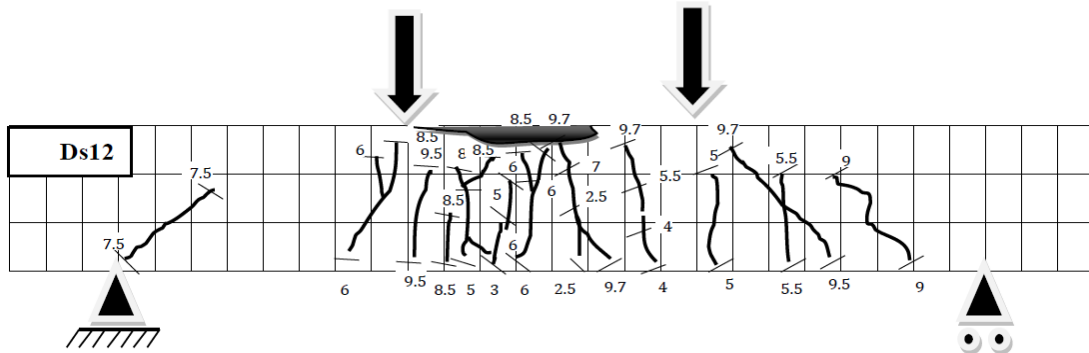


Fig. (9): Crack pattern of beam (Ds12)



Fig. (10): Shape of failure of beam (Ds12)

Group E

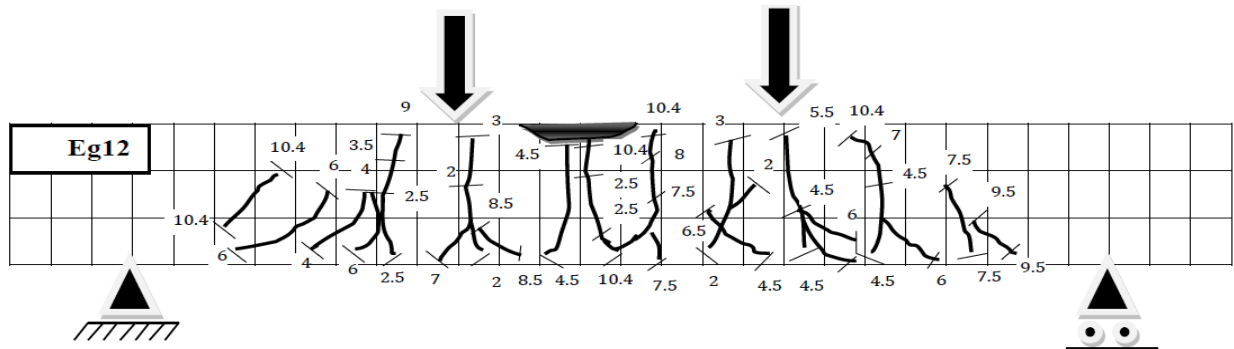


Fig. (11): Crack pattern of beam (Eg12)



Fig. (12): Shape of failure of beam (Eg12)

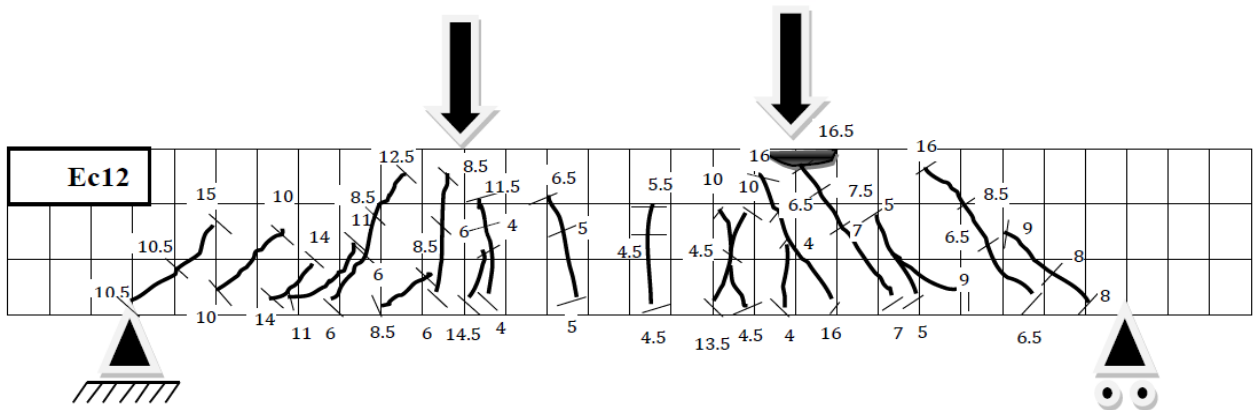


Fig. (13): Crack pattern of beam (Ec12)



Fig. (14): Shape of failure of beam (Ec12)

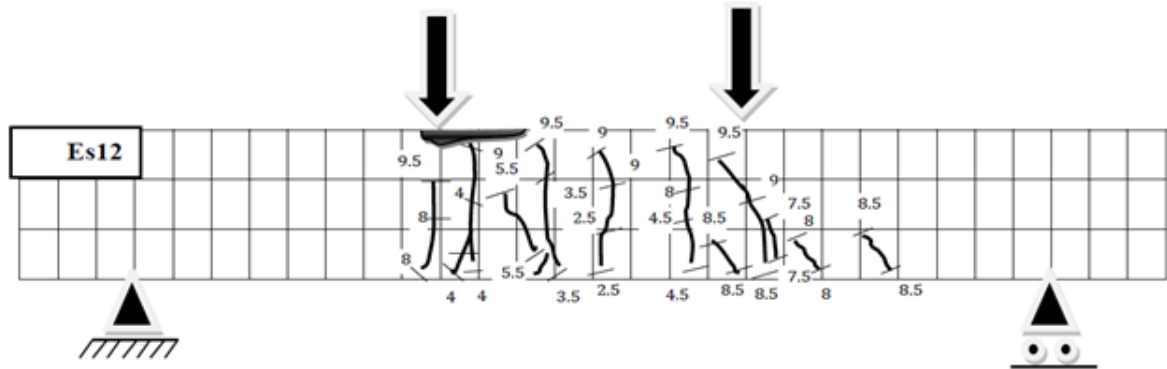


Fig. (15): Crack pattern of beam (Es12)

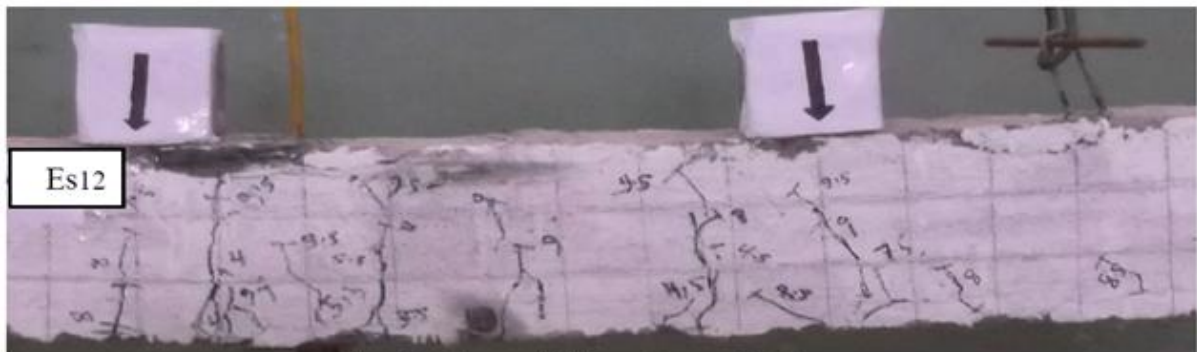


Fig. (16): Shape of failure of beam (Es12)

Group A

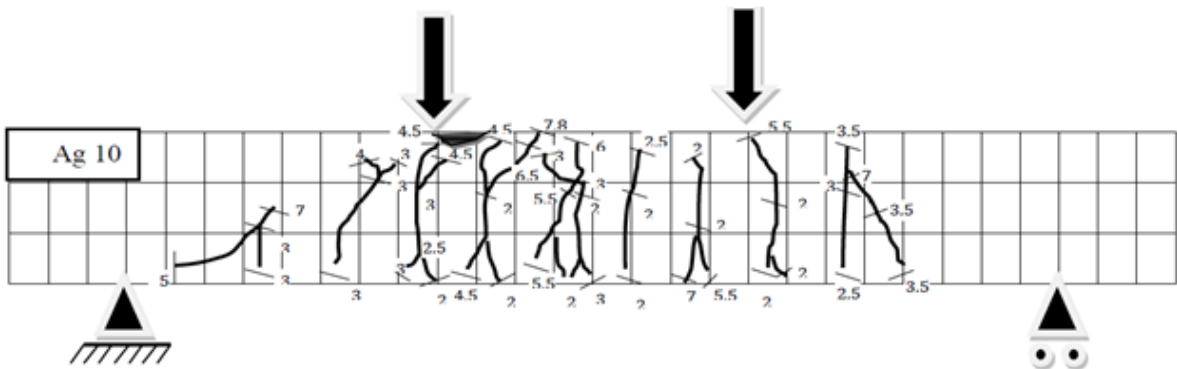


Fig. (17): Crack pattern of beam (Ag 10)



Fig. (18): Shape of failure of beam (Ag10)

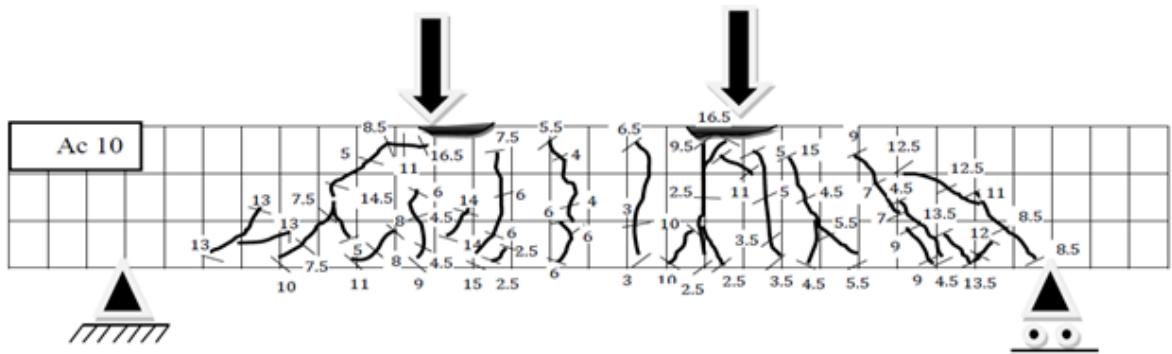


Fig. (19): Crack pattern of beam (Ac 10)



Fig. (20): Shape of failure of beam (Ac10)

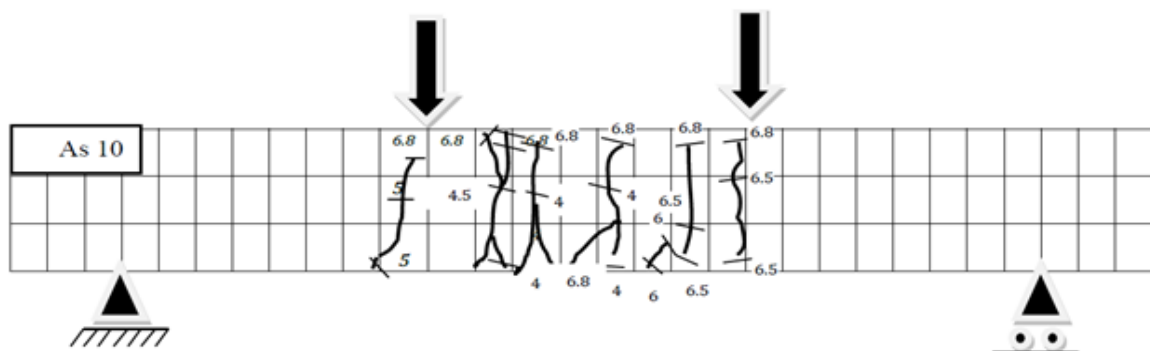


Fig. (21): Crack pattern of beam (As 10)



Fig. (22): Shape of failure of beam (As 10)

Group B

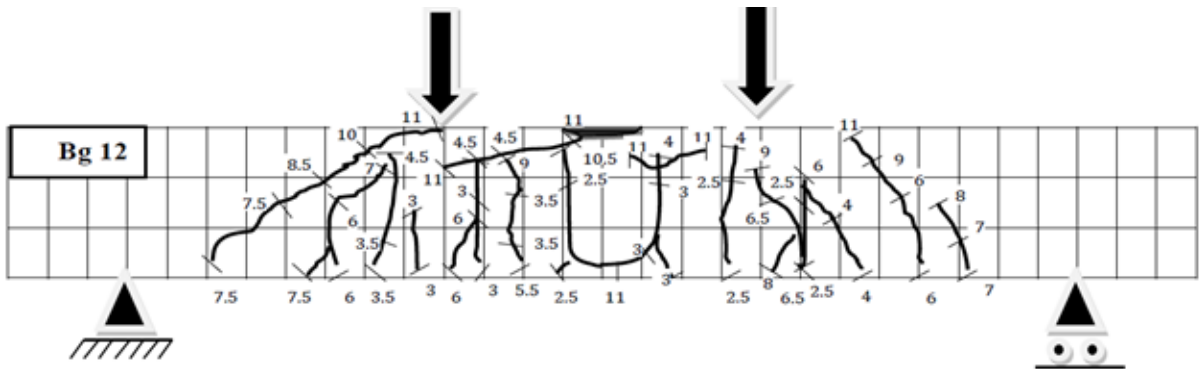


Fig. (23): Crack pattern of beam (Bg12)



Fig. (24): Shape of failure of beam (Bg12)

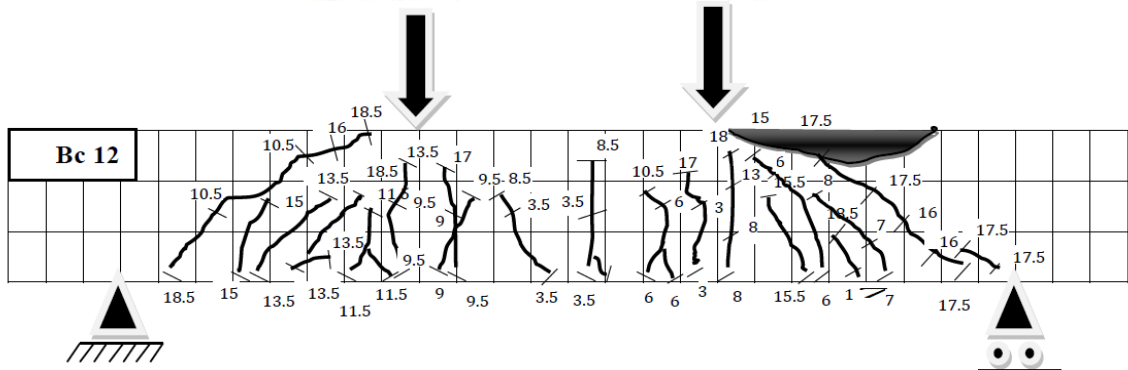


Fig. (25): Crack pattern of beam (Bc12)



Fig. (26): Shape of failure of beam (Bc12)

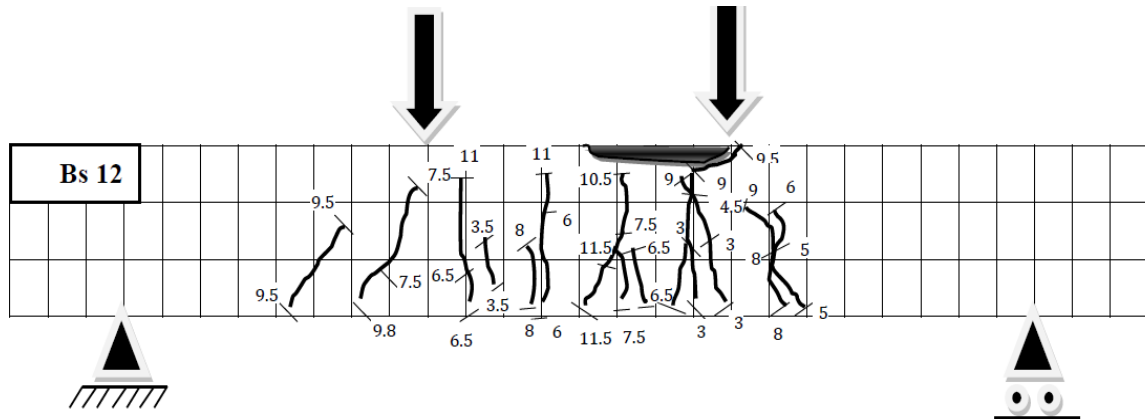


Fig. (27): Crack pattern of beam (BS 12)

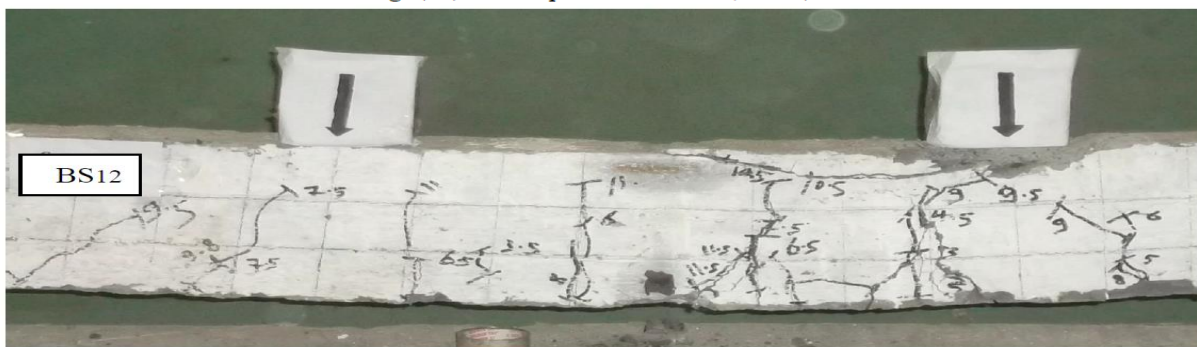


Fig. (28): Shape of failure of beam (BS12)

Group C

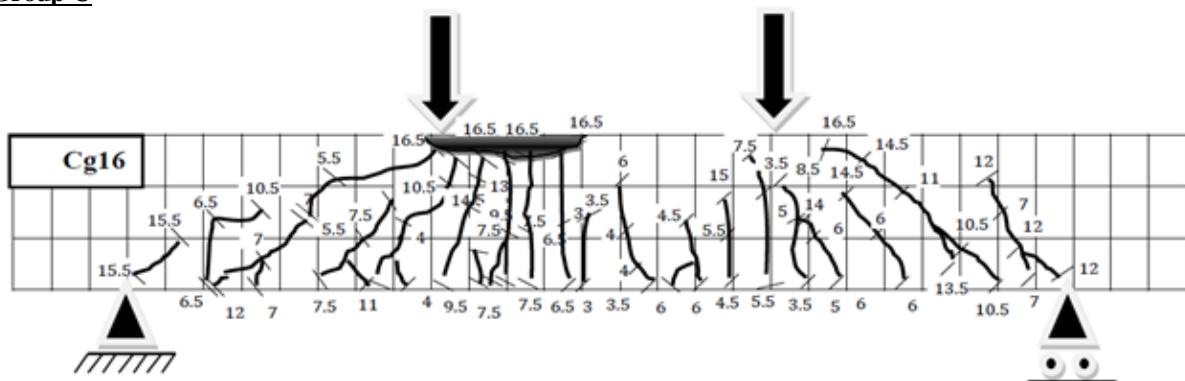


Fig. (29): Crack pattern of beam (Cg16)



Fig. (30): Shape of failure of beam (Cg16)

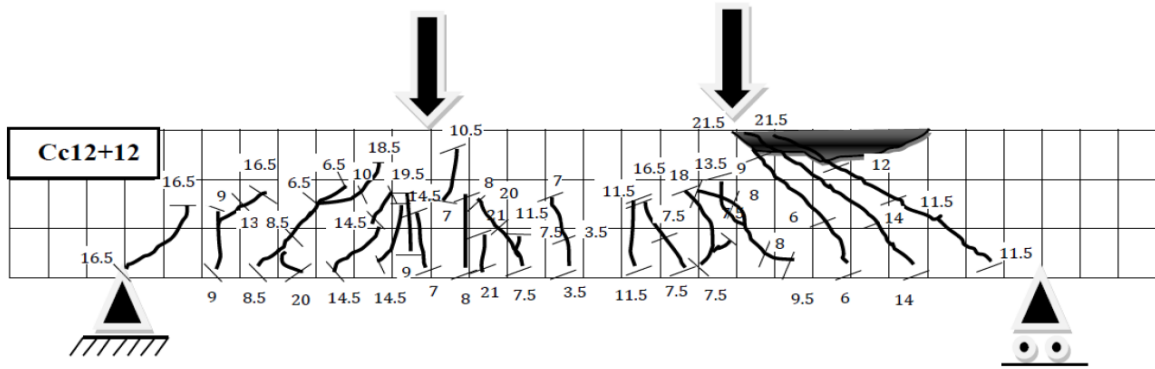


Fig. (31): Crack pattern of beam (Cc (12+12))

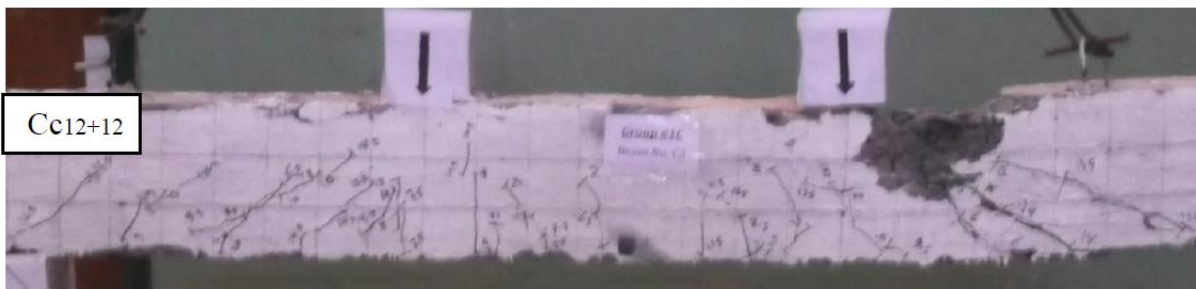


Fig. (32): Shape of failure of beam (Cc (12+12))

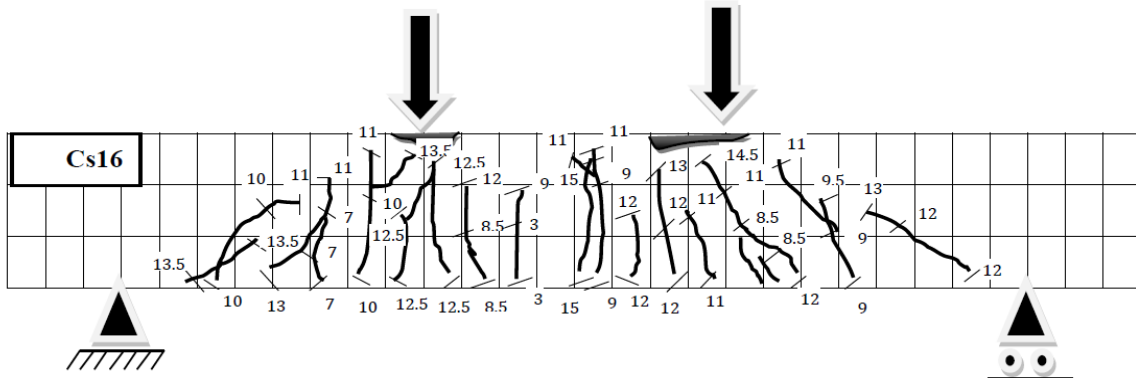


Fig. (33): Crack pattern of beam (Cs16)



Fig. (34): Shape of failure of beam (Cs16)

Table 7: Cracking (Pcr) and ultimate (Pu) loads for tested beams under static loads.

Group	Beam No.	Reinforcement type	b (cm)	d (cm)	Ar (cm ²)	fc (Kg/cm ²)	Pcr (ton)	Qsh (ton)	85% Pu (ton)	Pu (ton)	Mode of Failure
Group D	Dg12	GFRP	12	30	2Ø13	400	2	3	9.35	11	Flexural-Comp.
	Dc12	CFRP	12	30	2Ø13	400	2.5	6	12.6	14.8	Shear-Comp.
	Ds12	Steel	12	30	2Ø12	400	2.5	6	8.16	9.6	Flexural-Comp.
Group E	Eg12	GFRP	12	30	2Ø13	650	2.2	3.5	9.9	11.5	Flexural-Comp.
	Ec12	CFRP	12	30	2Ø13	650	2.8	7	14.28	16.8	Shear-Comp.
	Es12	Steel	12	30	2Ø12	650	2.7	6.5	8.5	10	Flexural-Comp.
Group A	Ag10	GFRP	12	30	2Ø 9	900	2	3.5	6.63	7.8	Flexural
	Ac10	CFRP	12	30	2Ø 9	900	3	7.5	14	16.5	Shear-Comp.
	As10	Steel	12	30	2Ø10	900	3	5.5	5.78	6.8	Flexural
Group B	Bg12	GFRP	12	30	2Ø13	900	2.5	4	10.2	12	Flexural-Comp.
	Bc12	CFRP	12	30	2Ø13	900	3	8	15.7	18.5	Shear-Comp.
	Bs12	Steel	12	30	2Ø12	900	3	7.5	9.8	11.5	Flexural-Comp.
Group C	Cg16	GFRP	12	30	2Ø16	900	3	4.5	14	16.5	Flexural-Comp.
	Cc(12+12)	CFRP	12	30	4Ø13	900	3.5	8.5	18.3	21.5	Shear-Comp.
	Cs16	Steel	12	30	2Ø16	900	3	8	12.75	15	Flexural-Comp.

3.2 Deflection characteristics

The measured values of maximum deflection are plotted versus the applied load from starting the loading up to failure as shown in Fig. (35), it mentioned 9 beams have changing in concrete strength value $f_c = 400, 650, 900$ by the same A_g & A_c & A_s and Fig.(36) it mentioned 9 beams have changing in A_g & A_c & A_s by The same concrete mix (high performance concrete ($f_c = 900 \text{ Kg/cm}^2$)). All plotted values indicated that, the deflection increases as the applied load increases.

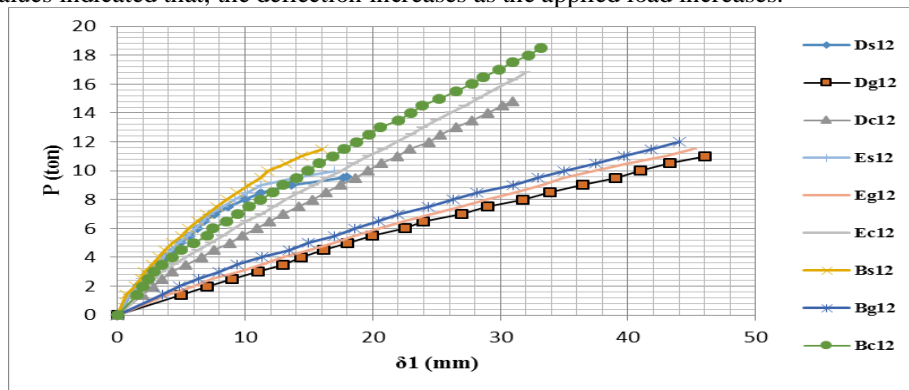


Fig. (35) Load-mid span deflection for beams group B, D, E

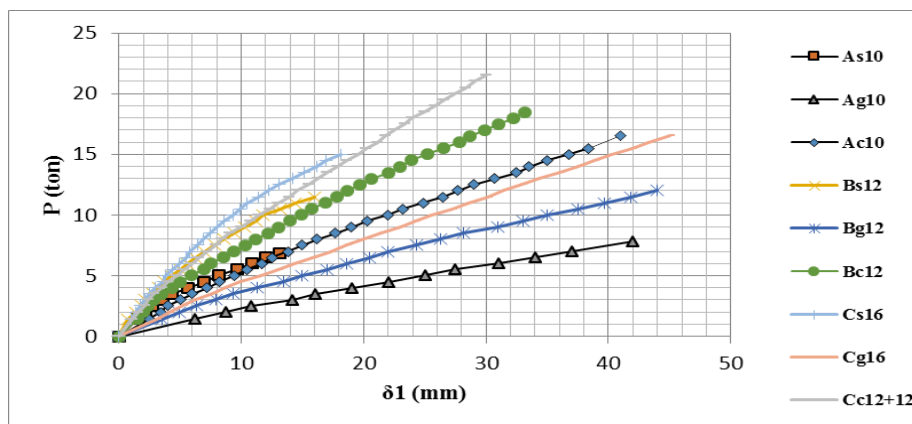


Fig. (36) Load-mid span deflection for beams group A, B, C

3.3 Concrete Strain Distribution.

Figure (37), (38) shows the behavior of the concrete strain in compression for all beams. The results indicated that all specimens presented almost have the same trend whereas the load increased, the strain also increased.

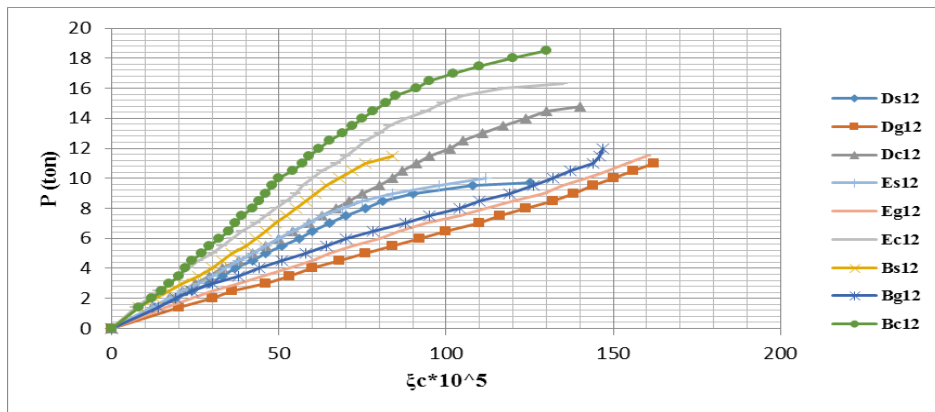


Fig. (37) Concrete Strain Distribution for beams tested group D, B, C

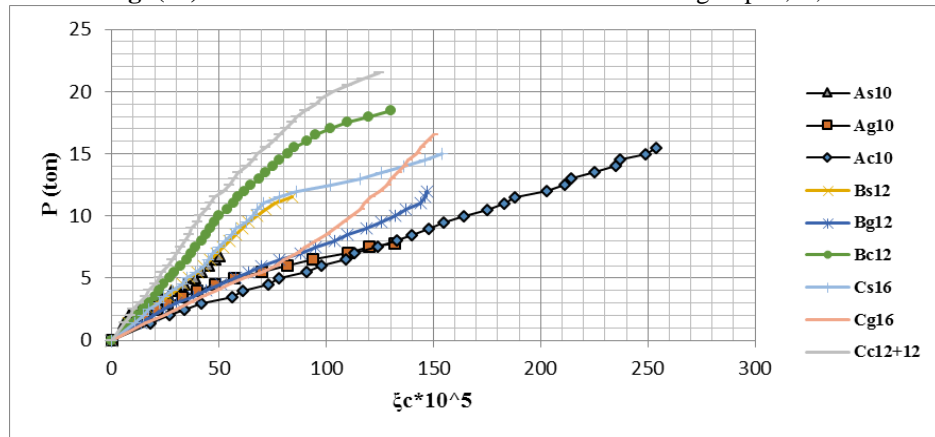


Fig. (38) Concrete Strain Distribution for beams tested group A, B, C.

3.4 Steel Strain Distribution

Figure (39), (40) shows the behavior of the steel strain in compression for all beams. The results indicated that all specimens presented almost have the same trend whereas the load increased, the strain also increased.

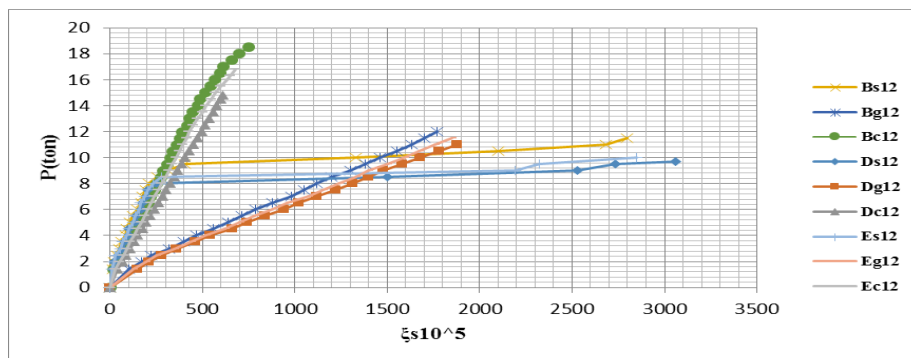


Fig. (39) Steel Strain Distribution for beams tested group B, D, E

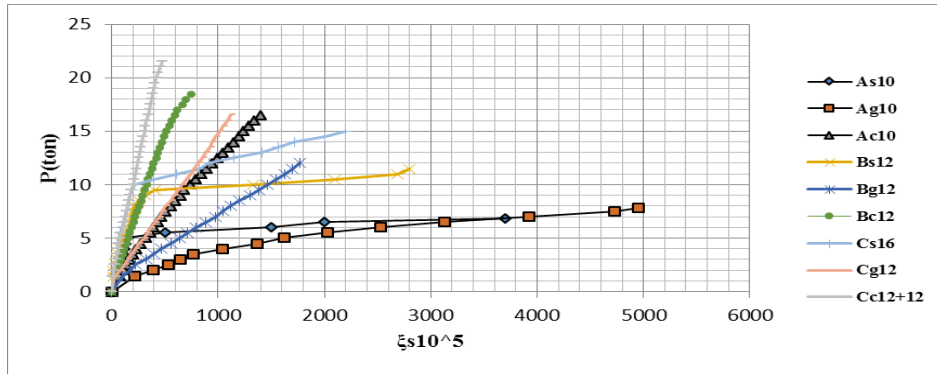


Fig. (40) Steel Strain Distribution for beams tested group A, B, C.

3.5 Load –Slip relationship for the beams

The end slip is plotted against the applied load from the starting of loading up to failure as shown in fig. (41)&fig. (42).

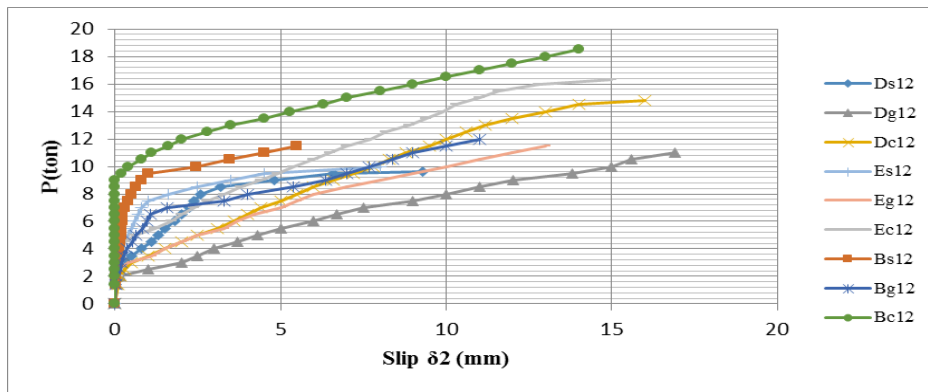


Fig. (41) End Slip Distribution for beams tested group B, D, E

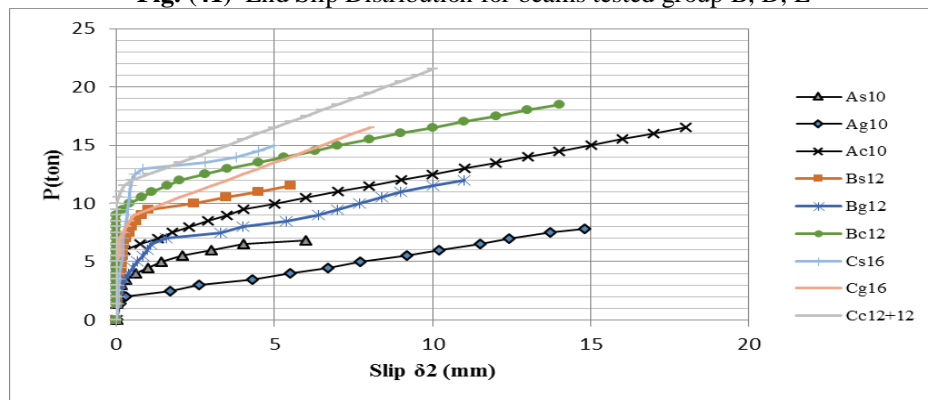


Fig. (42) End Slip Distribution for beams tested group A, B, C.

IV. Discussion of Test Result

This item describes and interprets the analysis of the obtained test results of the tested beams. The analysis includes the relationship between the value of cracking , shear and ultimate loads, deflection, concrete strain, steel strain and end slip for tested beams as given in table (8) to (11).The value of crack and ultimate load in experimental compared by theoretical values were mentioned in table (12)

Table (8): Values of the deflection at cracking, shear and ultimate load for tested beams.

Group	Beam No.	Reinforcement type	b (cm)	d (cm)	Ar (cm ²)	f _c (Kg/cm ²)	δ _{1cr} (mm)	δ _{1sh} (mm)	85% δ _{1u} (mm)	δ _{1u} (mm)
Group D	Dg12	GFRP	12	30	2Ø13	400	7	11	40	47.5
	Dc12	CFRP	12	30	2Ø13	400	3.5	11	25.5	31
	Ds12	Steel	12	30	2Ø12	400	2.3	6.25	10	18
Group E	Eg12	GFRP	12	30	2Ø13	650	6.6	11.3	37	45
	Ec12	CFRP	12	30	2Ø13	650	3.1	11.1	26.5	32
	Es12	Steel	12	30	2Ø12	650	2.2	6.7	10.3	17
Group A	Ag10	GFRP	12	30	2Ø 9	900	8.69	16	35	42
	Ac10	CFRP	12	30	2Ø 9	900	5	15	33.5	41
	As10	Steel	12	30	2Ø10	900	3.55	9.7	10.4	13.1
Group B	Bg12	GFRP	12	30	2Ø13	900	6.35	11.35	36	44
	Bc12	CFRP	12	30	2Ø13	900	2.87	11.2	27	33.2
	Bs12	Steel	12	30	2Ø12	900	2.13	7.8	11.6	16
Group C	Cg16	GFRP	12	30	2Ø16	900	6.25	9.95	38	45
	Cc(12+12)	CFRP	12	30	4Ø13	900	2.9	9.1	25	30
	Cs16	Steel	12	30	2Ø16	900	2.09	6.89	13.8	18.1

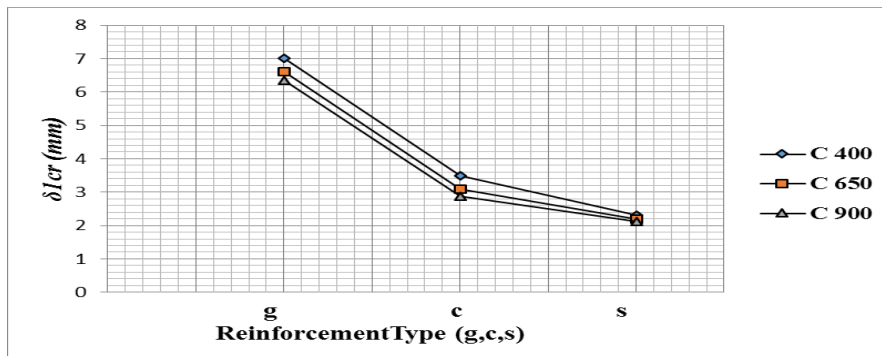


Fig. (43): The deflection at cracking load versus reinforcement type

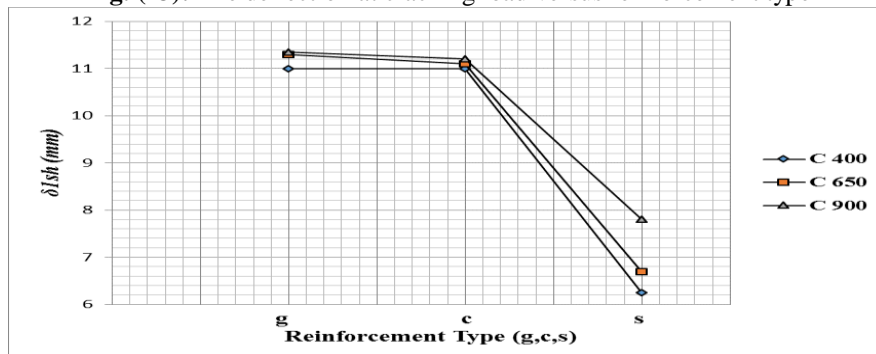


Fig. (44): The deflection at shear load (δ_{1sh}) versus reinforcement type

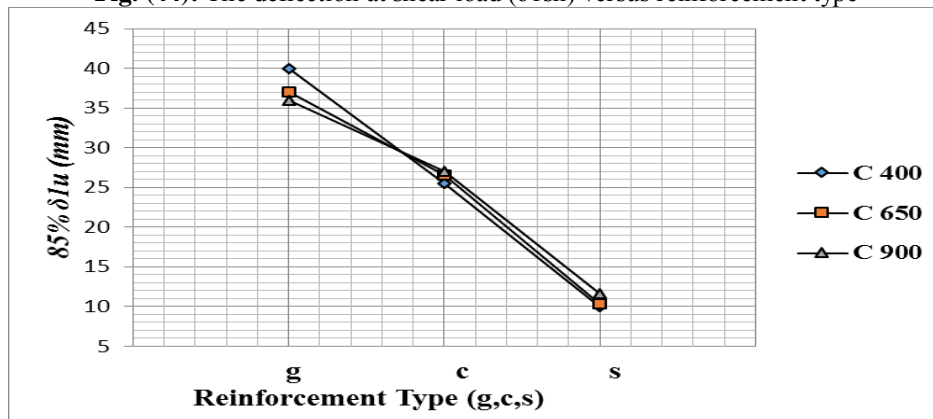


Fig. (45): The deflection at 85% ultimate load (δ_{1u}) versus reinforcement type

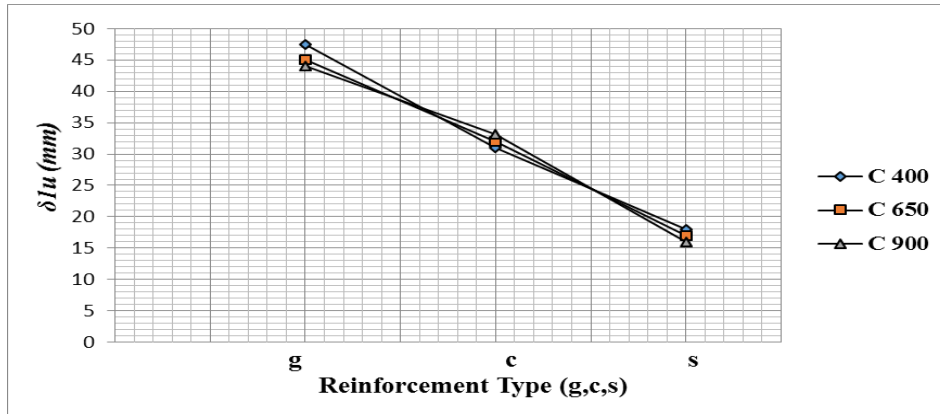


Fig.(46): The deflection at ultimate load (δ_{1u}) versus reinforcement type.

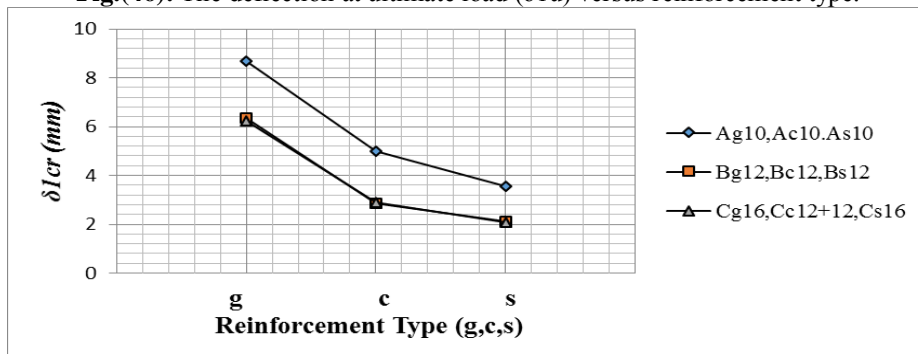


Fig. (47): Deflection at crack load versus reinforcement type

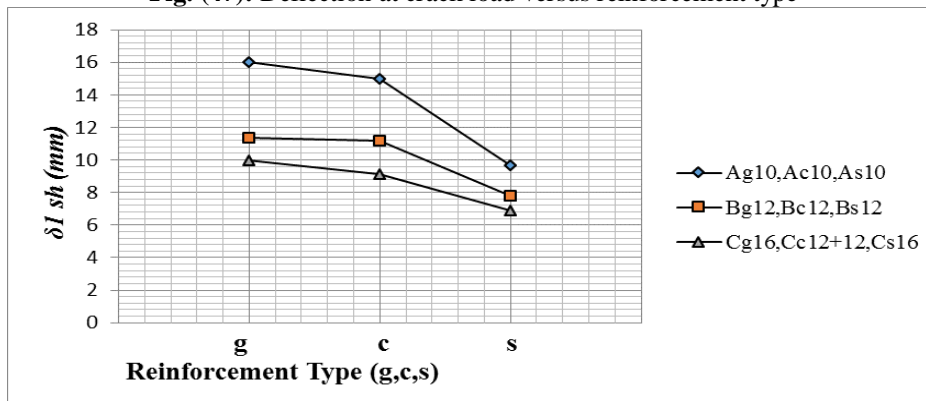


Fig. (48): Deflection at shear load versus reinforcement type.

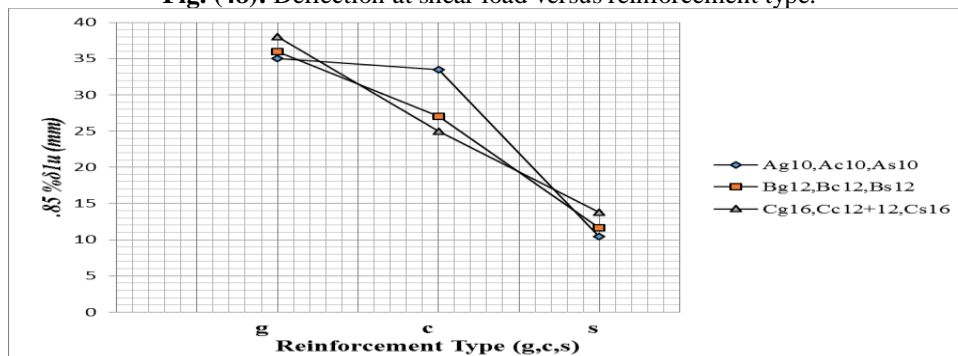


Fig. (49): Deflection at 85% ultimate load versus reinforcement type.

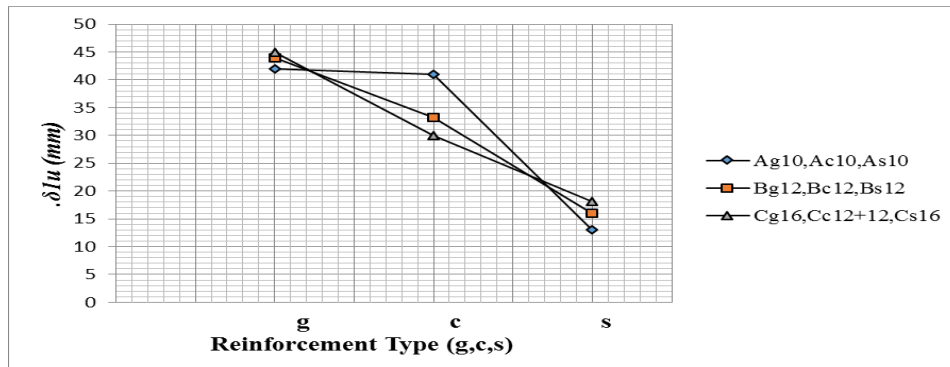


Fig. (50): Deflection at ultimate load versus reinforcement type.

Table (9): Values of concrete strain at cracking, shear, 85% ultimate and ultimate load for tested beams.

Group	Beam No.	Reinforcement type	b (cm)	d (cm)	Ar (cm ²)	fc (Kg/cm ²)	$\xi_{c cr} * 10^{-5}$	$\xi_{c sh} * 10^{-5}$	85% $\xi_{c u} * 10^{-5}$	$\xi_{c u} * 10^{-5}$
Group D	Dg12	GFRP	12	30	2Ø13	400	30	46	148	166
	Dc12	CFRP	12	30	2Ø13	400	21	50	106	140
	Ds12	Steel	12	30	2Ø12	400	24	56	77	125
Group E	Eg12	GFRP	12	30	2Ø13	650	28	45	140	160
	Ec12	CFRP	12	30	2Ø13	650	18	43	92	135
	Es12	Steel	12	30	2Ø12	650	23	54	75	112
Group A	Ag10	GFRP	12	30	2Ø9	900	15	33	96	132
	Ac10	CFRP	12	30	2Ø9	900	42	124	235	254
	As10	Steel	12	30	2Ø10	900	18	42	44	50
Group B	Bg12	GFRP	12	30	2Ø13	900	24	44	133	147
	Bc12	CFRP	12	30	2Ø13	900	17	42	89	130
	Bs12	Steel	12	30	2Ø12	900	21	52	67	84
Group C	Cg16	GFRP	12	30	2Ø16	900	36	55	136	150
	Cc(12+12)	CFRP	12	30	4Ø13	900	16	36	87	125
	Cs16	Steel	12	30	2Ø16	900	22	53	112	154

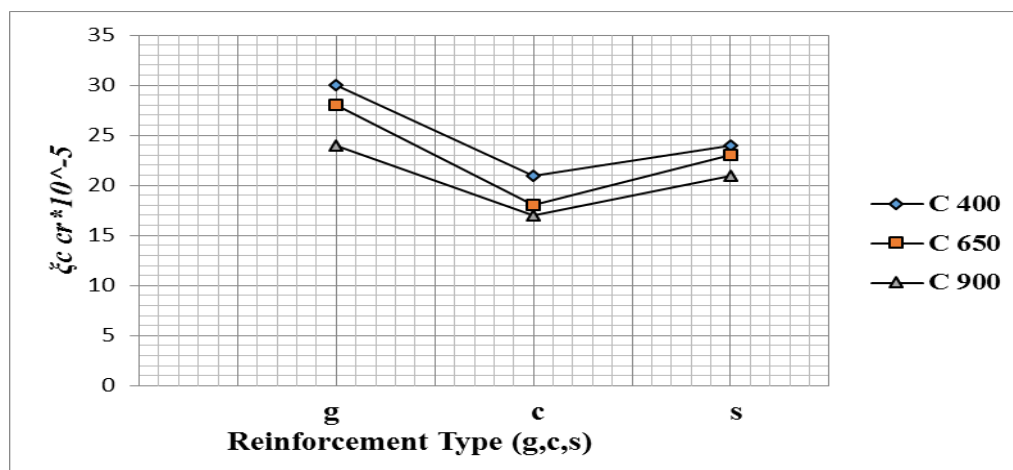


Fig. (51): The concrete strain at cracking load versus reinforcement type.

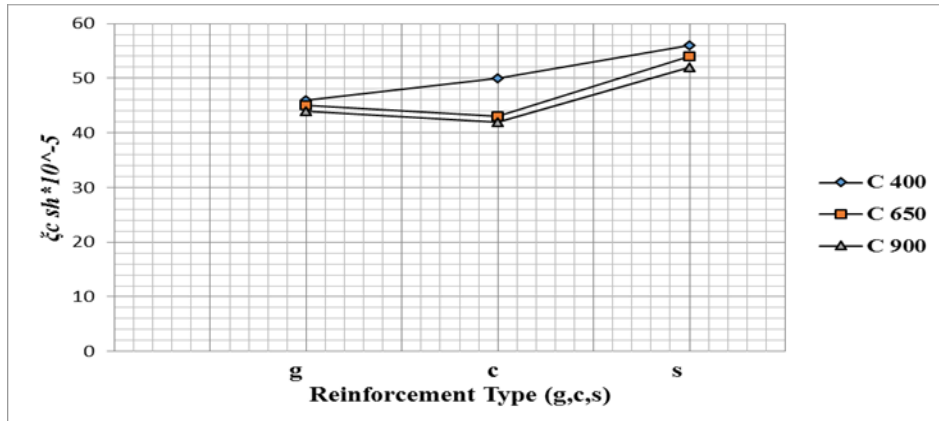


Fig. (52): The concrete strain at shear load versus reinforcement type.

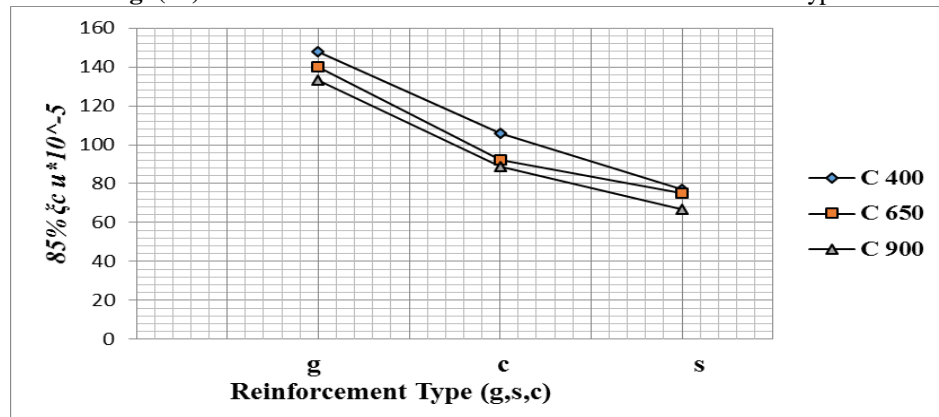


Fig. (53): The concrete strain at 85% ultimate load ($\xi_{c u}$) versus reinforcement type.

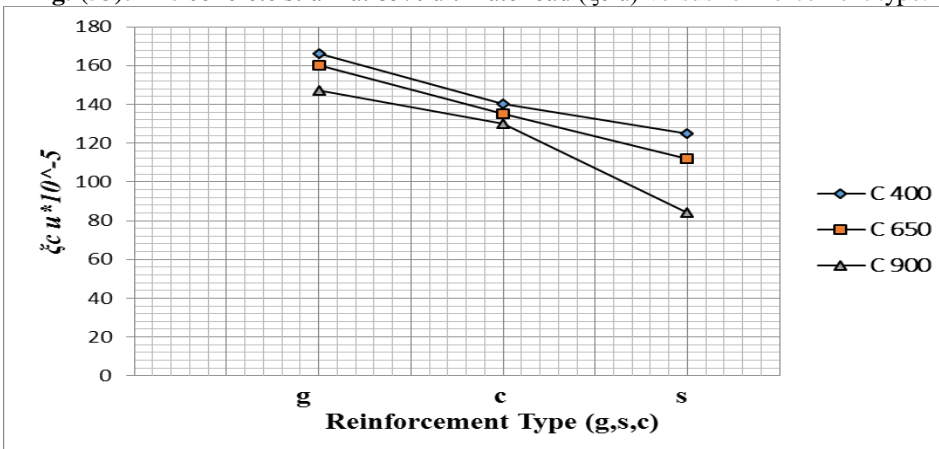


Fig. (54): The concrete strain at ultimate load ($\xi_{c u}$) versus reinforcement type.

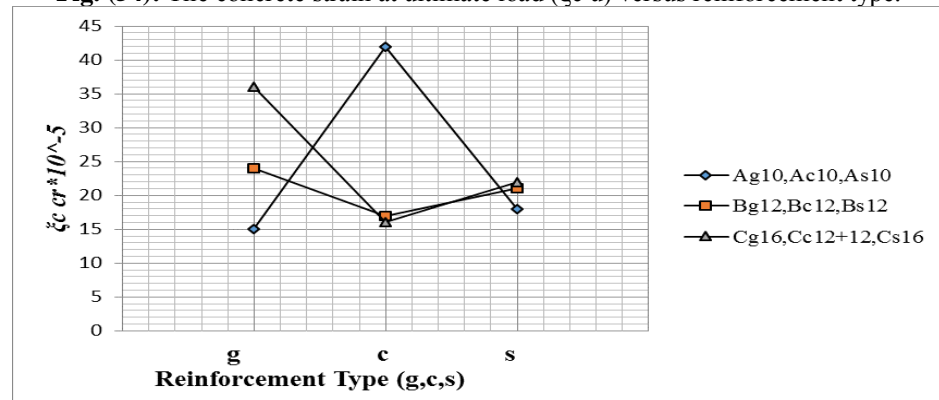


Fig. (55): Concrete strain at crack load versus reinforcement type.

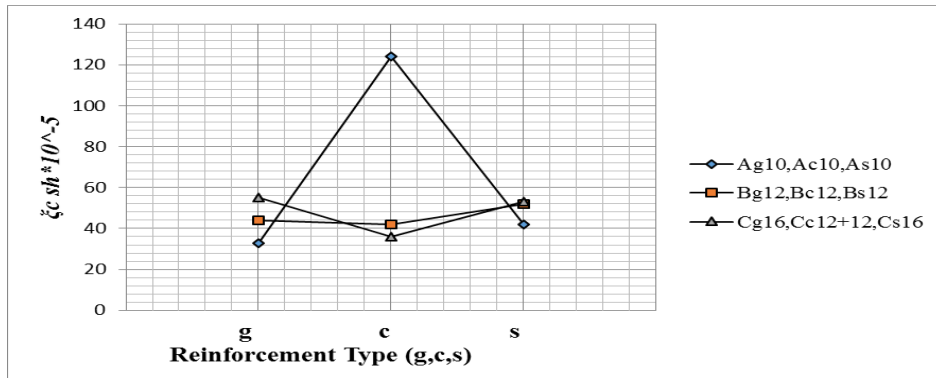


Fig. (56): Concrete strain at shear load versus reinforcement type.

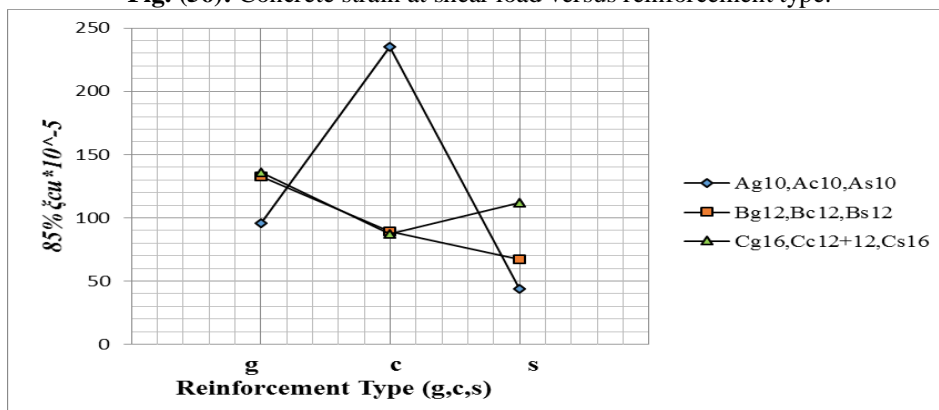


Fig. (57): Concrete strain at 85% ultimate load versus reinforcement type.

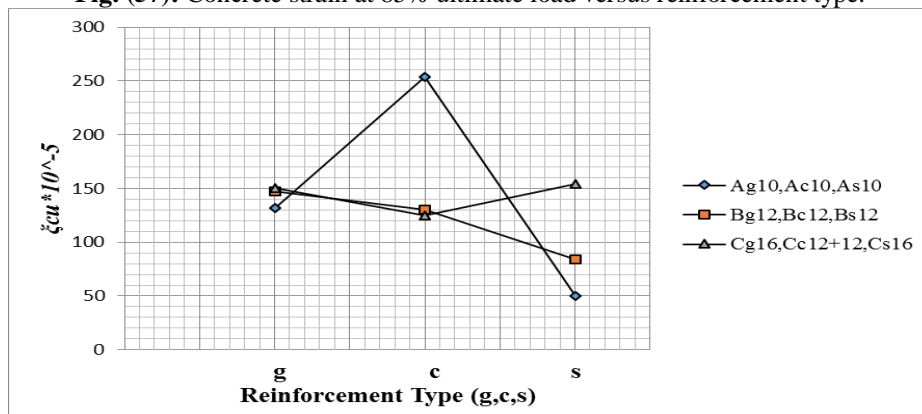


Fig. (58): Concrete strain at ultimate load versus reinforcement type.

Table (10): Values of reinforcement strain at cracking, shear, 85% ultimate and ultimate load for tested beams.

Group	Beam No.	Reinforcement type	b (cm)	d (cm)	Ar (cm ²)	fc (Kg/cm ²)	$\xi_{r cr} * 10^5$	$\xi_{r sh} * 10^5$	85% $\xi_{r u} * 10^5$	$\xi_{r u} * 10^5$
Group D	Dg12	GFRP	12	30	2Ø13	400	210	360	1640	1940
	Dc12	CFRP	12	30	2Ø13	400	84	238	520	610
	Ds12	Steel	12	30	2Ø12	400	44	169	700	3058
Group E	Eg12	GFRP	12	30	2Ø13	650	217	440	1554	1850
	Ec12	CFRP	12	30	2Ø13	650	82	240	532	680
	Es12	Steel	12	30	2Ø12	650	46	175	1000	2850
Group A	Ag10	GFRP	12	30	2Ø9	900	390	765	3300	4950
	Ac10	CFRP	12	30	2Ø9	900	166	507	1140	1400
	As10	Steel	12	30	2Ø10	900	95	500	1500	3700
Group B	Bg12	GFRP	12	30	2Ø13	900	220	470	1496	1770
	Bc12	CFRP	12	30	2Ø13	900	81	255	555	750
	Bs12	Steel	12	30	2Ø12	900	50	195	1300	2800
Group C	Cg16	GFRP	12	30	2Ø16	900	155	250	950	1120
	Cc(12+12)	CFRP	12	30	4Ø13	900	50	160	381	480
	Cs16	Steel	12	30	2Ø16	900	37	147	1250	2200

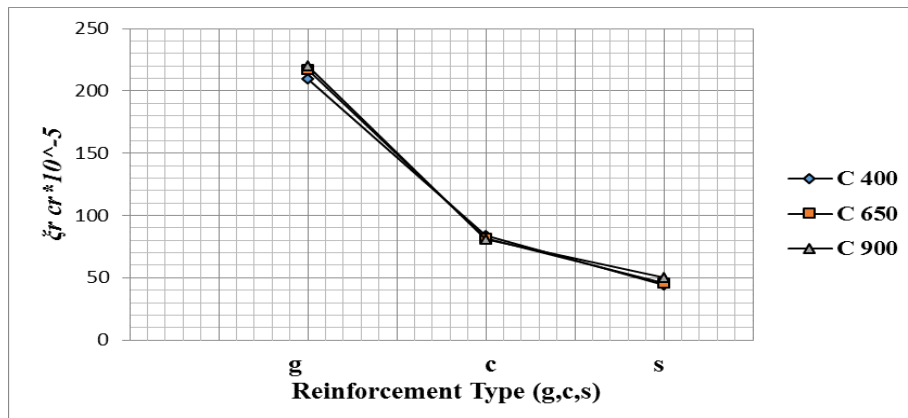


Fig. (59): The reinforcement strain at cracking load versus reinforcement type.



Fig. (60): The reinforcement strain at shear load (ξ_{rsh}) versus reinforcement type.

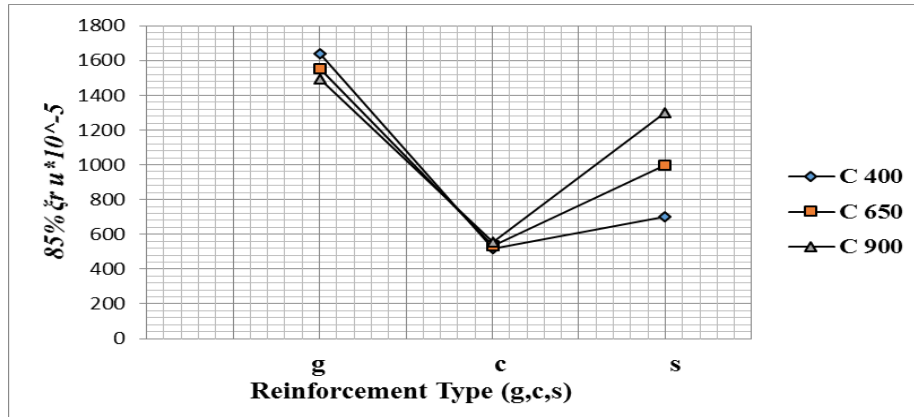


Fig. (61): Reinforcement strain at 85% ultimate load ($\xi_r u$) versus reinforcement type.

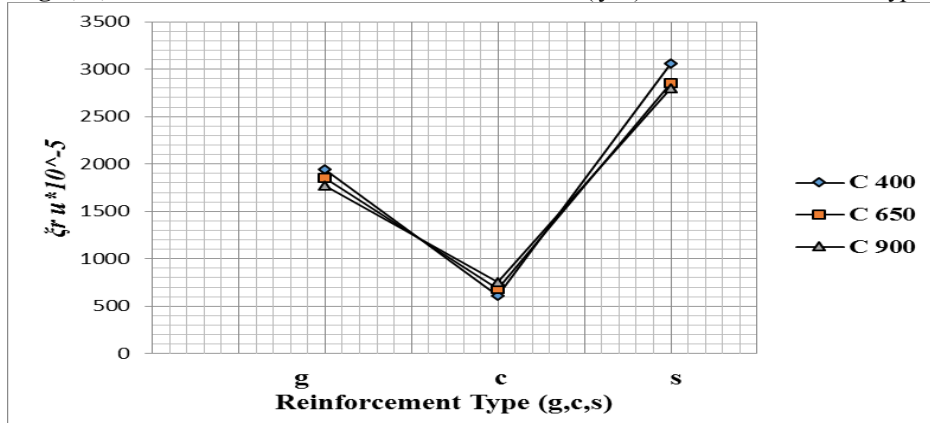


Fig. (62): Reinforcement strain at ultimate load ($\xi_r u$) versus reinforcement type.

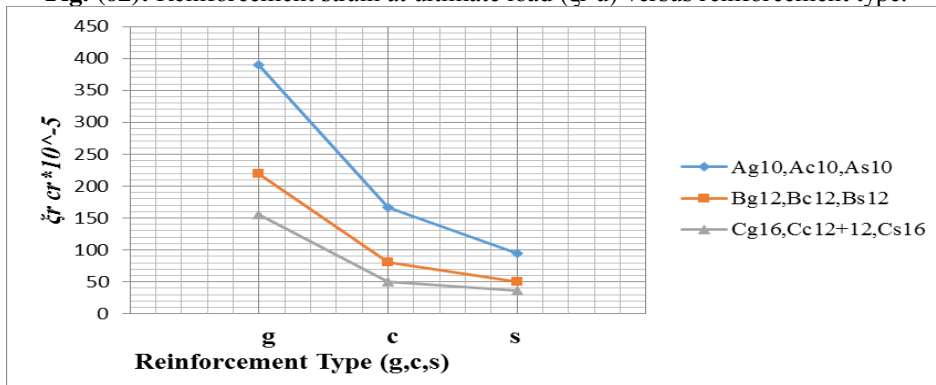


Fig. (63): Reinforcement strain at crack load (ξ_{rcr}) versus reinforcement type.

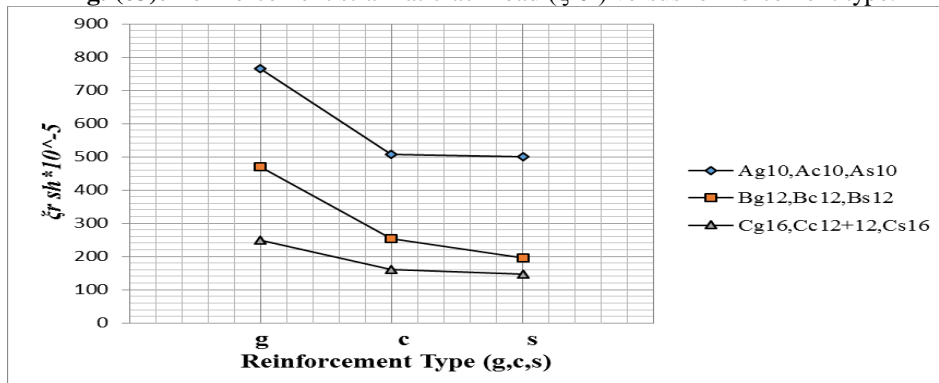


Fig. (64): Reinforcement strain at shear load (ξ_{rsh}) versus reinforcement type.

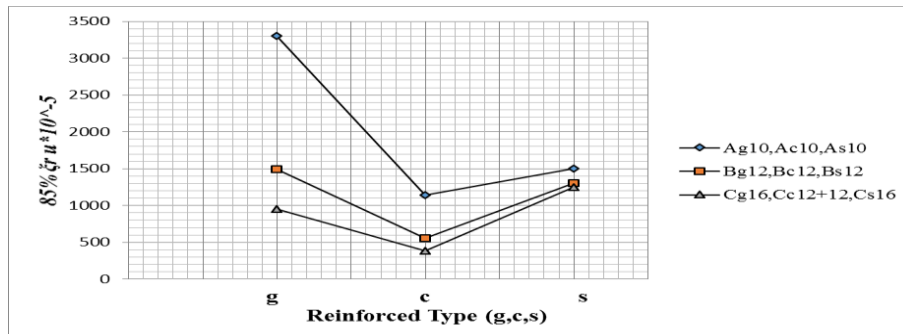


Fig. (65): Reinforcement strain at 85% ultimate load versus reinforcement type.

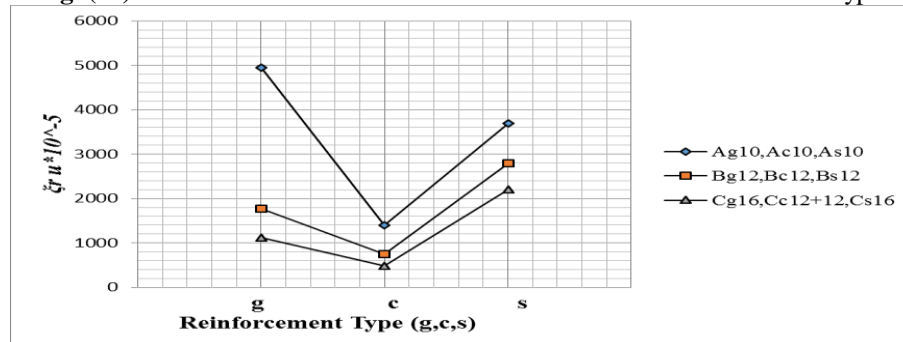


Fig. (66): Reinforcement strain at ultimate load versus reinforcement type.

Table (11): Values of main reinforcement bars slip at cracking, shear, 85% of the ultimate and ultimate load for tested beams.

Group	Beam No.	Reinforcement type	b (cm)	d (cm)	Ar (cm ²)	fc (Kg/cm ²)	δ2cr (mm)	δ2sh (mm)	85% δ2u (mm)	δ2u (mm)
Group D	Dg12	GFRP	12	30	2Ø13	400	0.3	2	12.9	16.92
	Dc12	CFRP	12	30	2Ø13	400	0.2	3.6	11	16
	Ds12	Steel	12	30	2Ø12	400	0.2	1.8	2.73	9.3
Group E	Eg12	GFRP	12	30	2Ø13	650	0.2	1.1	9.8	13
	Ec12	CFRP	12	30	2Ø13	650	0.1	2	10.1	15
	Es12	Steel	12	30	2Ø12	650	0.15	0.7	2.5	8
Group A	Ag10	GFRP	12	30	2Ø9	900	0.3	4.3	11.7	14.8
	Ac10	CFRP	12	30	2Ø9	900	0	1.76	13	18
	As10	Steel	12	30	2Ø10	900	0.15	2.08	3	6
Group B	Bg12	GFRP	12	30	2Ø13	900	0.15	0.38	7.97	11
	Bc12	CFRP	12	30	2Ø13	900	0	0	8.4	14
	Bs12	Steel	12	30	2Ø12	900	0.1	0.4	2	5.5
Group C	Cg16	GFRP	12	30	2Ø16	900	0	0	5.5	8
	Cc(12+12)	CFRP	12	30	4Ø13	900	0	0	6.75	10
	Cs16	Steel	12	30	2Ø16	900	0.07	0.26	0.72	5

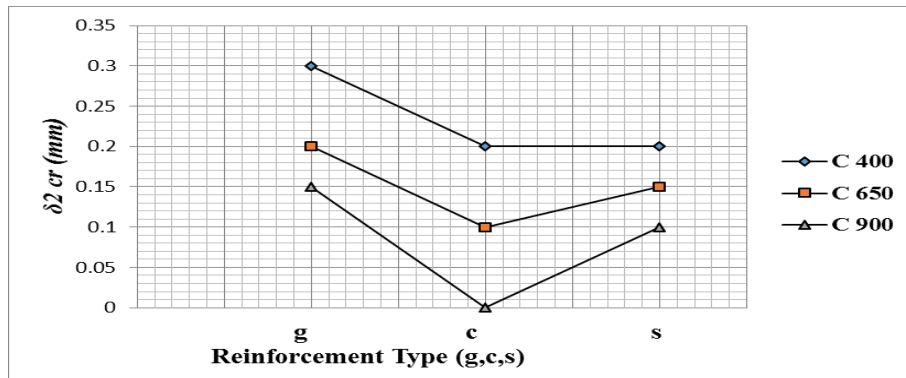


Fig. (67): Slip of main reinforcement at crack load ($\delta 2 cr$) versus reinforcement type.

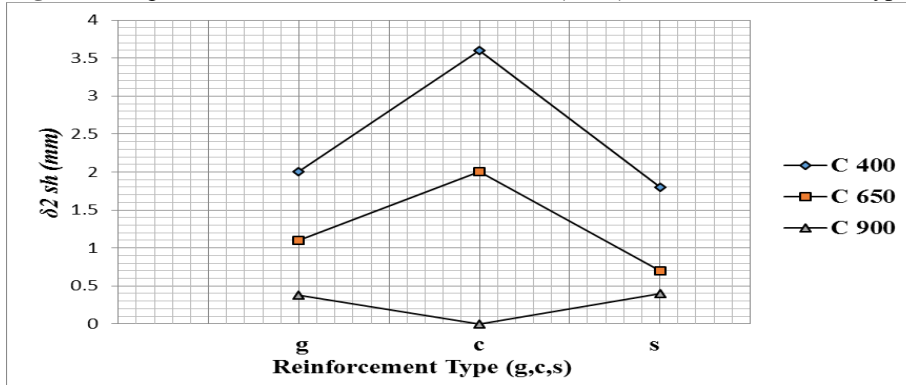


Fig. (68): Slip of main reinforcement at shear load ($\delta 2 sh$) versus reinforcement type.

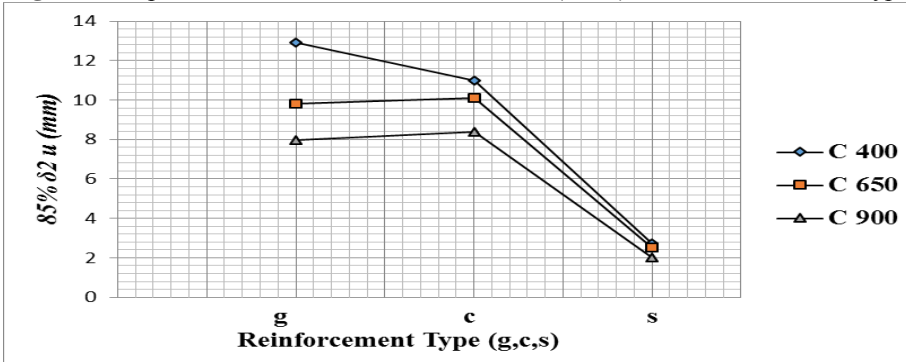


Fig. (69): Slip of main reinforcement at 85% ultimate load ($\delta 2 u$) versus reinforcement type

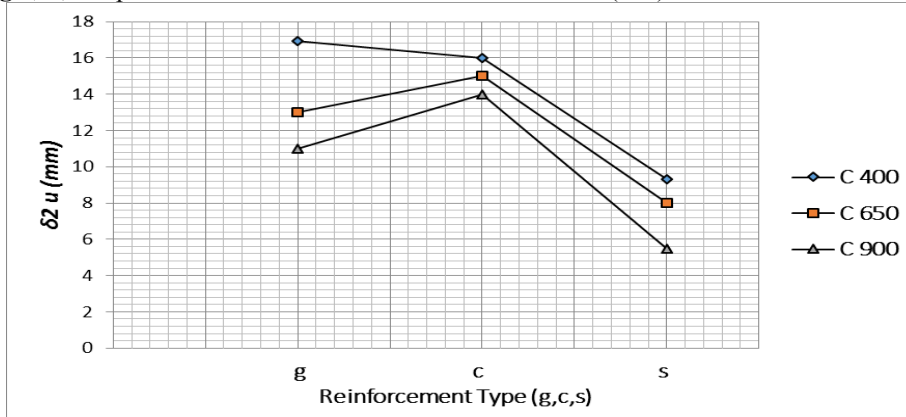


Fig. (70): Slip of main reinforcement at ultimate load ($\delta 2 u$) versus reinforcement type

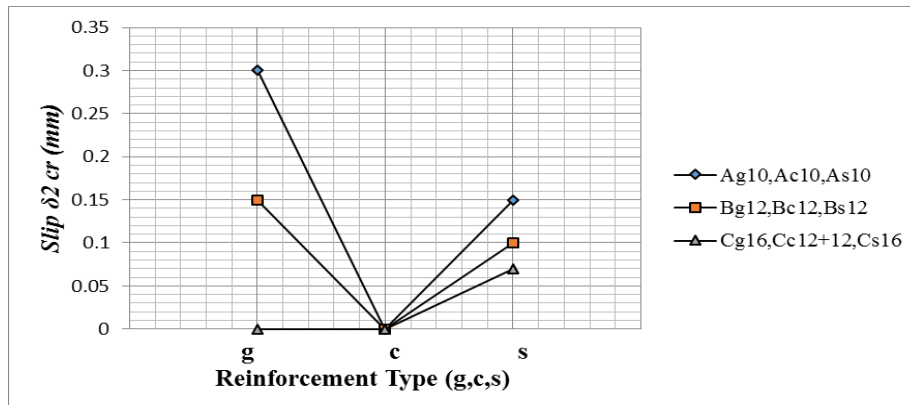


Fig. (71): Slip of main reinforcement at crack load versus reinforcement type.

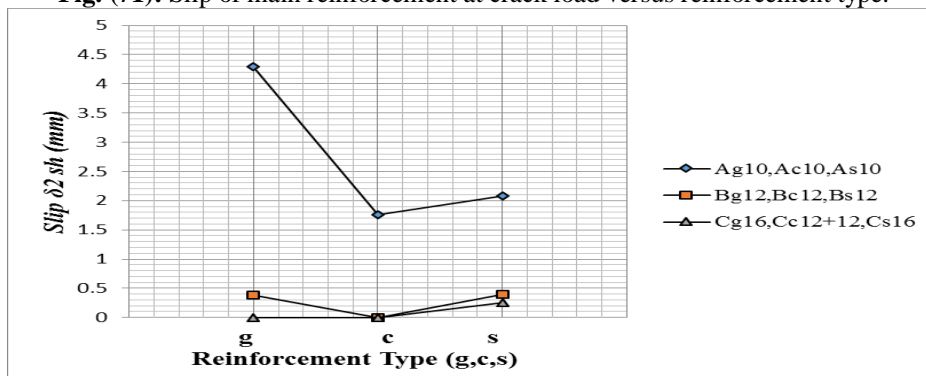


Fig. (72): Slip of main reinforcement at shear load versus reinforcement type.

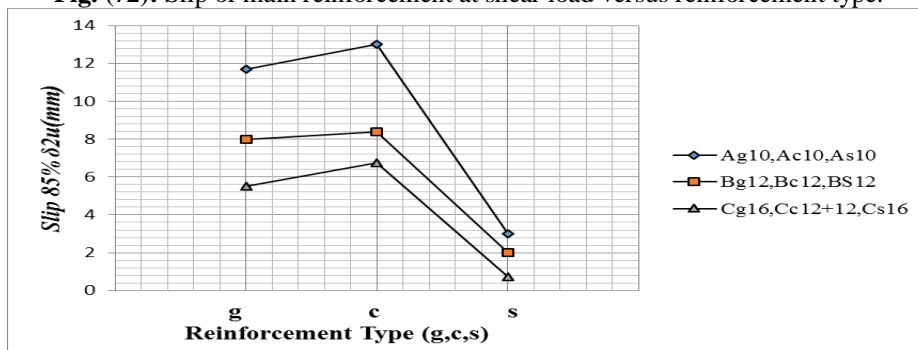


Fig. (73): Slip of main reinforcement at 85% ultimate load versus reinforcement type.

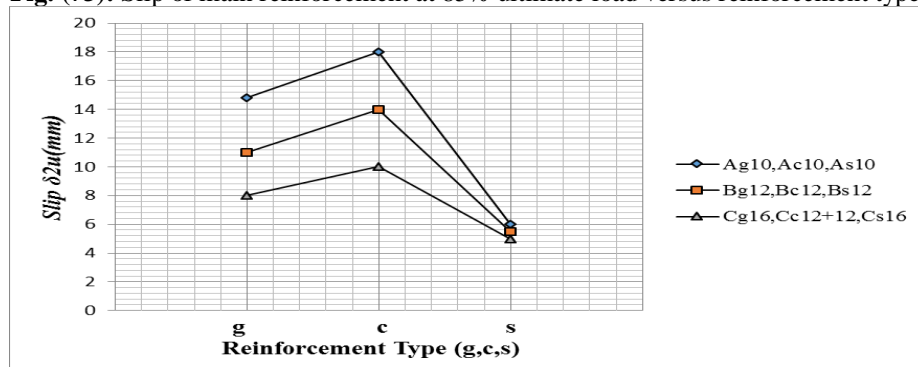


Fig. (74): Slip of main reinforcement at ultimate load versus reinforcement type.

Table (12): The value of crack and ultimate load in experimental compared by theoretical values.

Group	Beam No.	Reinforcement type	b (cm)	d (cm)	Ar (cm ²)	fc (Kg/cm ²)	Pcr experimental (ton)	Pcr theoretical (ton)	Pcr ex /Pcr th	Pu experimental (ton)	Pu theoretical (ton)	Pu ex /Pu th
Group D	Dg12	GFRP	12	30	2Ø13	400	2	2.4	0.83	11	1.95	5.64
	Dc12	CFRP	12	30	2Ø13	400	2.5	2.4	1.04	14.8	5.23	2.83
	Ds12	Steel	12	30	2Ø12	400	2.5	2.4	1.04	9.6	6.89	1.39
Group E	Eg12	GFRP	12	30	2Ø13	650	2.2	3.1	0.71	11.5	1.95	5.90
	Ec12	CFRP	12	30	2Ø13	650	2.8	3.1	0.90	16.8	7.2	2.33
	Es12	Steel	12	30	2Ø12	650	2.7	3.1	0.87	10	7	1.43
Group A	Ag10	GFRP	12	30	2Ø9	900	2	3.81	0.52	7.8	1.17	6.67
	Ac10	CFRP	12	30	2Ø9	900	3	3.81	0.79	16.5	5.77	2.86
	As10	Steel	12	30	2Ø10	900	3	3.81	0.79	6.8	4.92	1.38
Group B	Bg12	GFRP	12	30	2Ø13	900	2.5	3.81	0.66	12	1.95	6.15
	Bc12	CFRP	12	30	2Ø13	900	3	3.81	0.79	18.5	8.85	2.09
	Bs12	Steel	12	30	2Ø12	900	3	3.81	0.79	11.5	7.05	1.63
Group C	Cg16	GFRP	12	30	2Ø16	900	3	3.81	0.79	16.5	3.26	5.06
	Cc(12+12)	CFRP	12	30	4Ø13	900	3.5	3.81	0.92	21.5	11.52	1.87
	Cs16	Steel	12	30	2Ø16	900	3	3.81	0.79	15	12.1	1.24

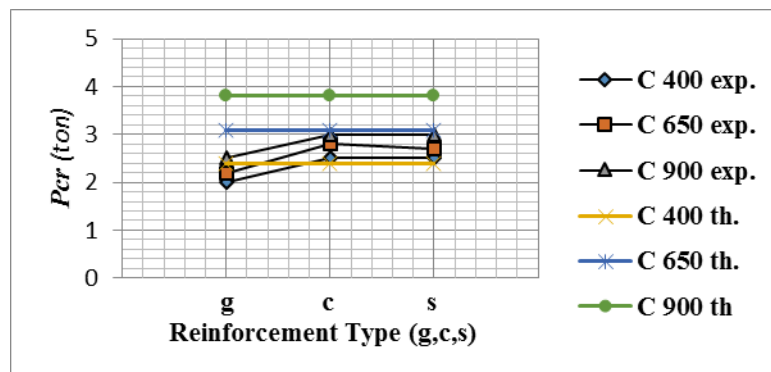


Fig. (75): Theoretical and experimental cracking load versus reinforcement type.

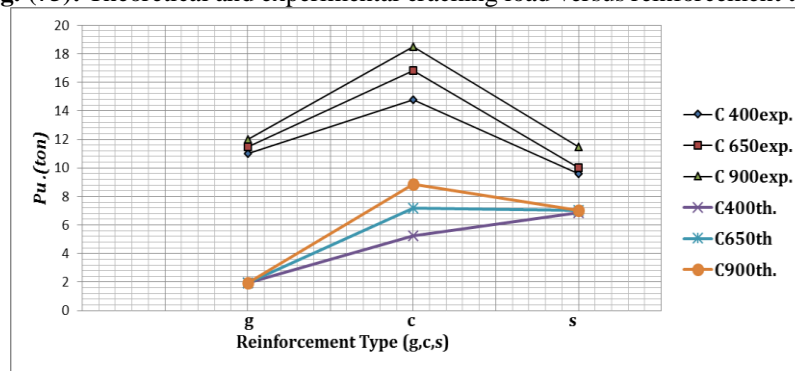


Fig. (76): Theoretical and experimental ultimate load versus reinforcement type.

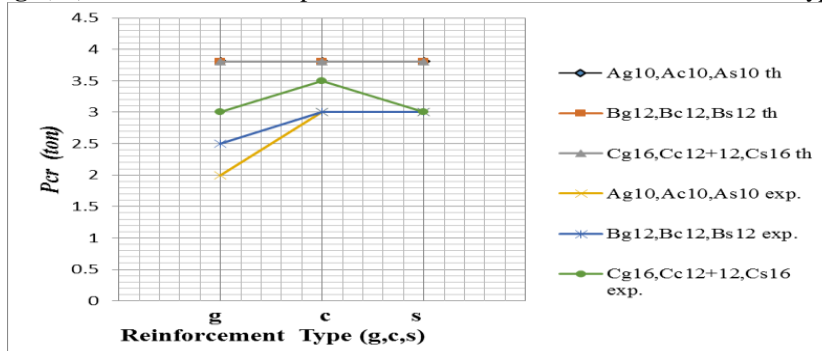


Fig. (77): Theoretical and experimental cracking load versus reinforcement type.

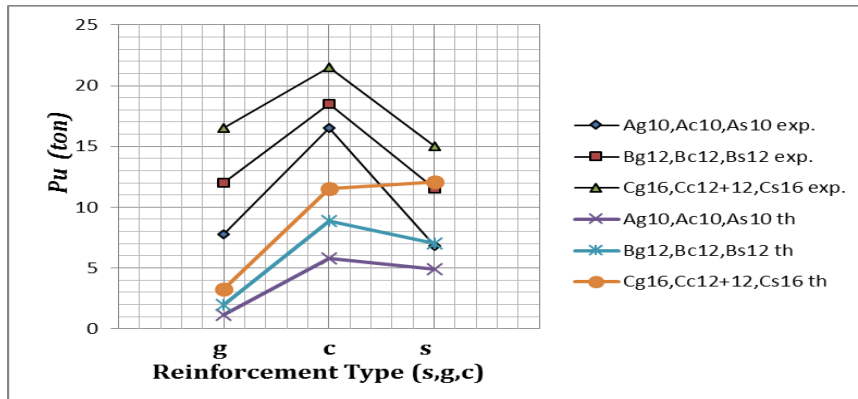


Fig. (78): Theoretical and experimental ultimate load versus reinforcement type

4.1 Failure mode compared between theoretical and experimental study.

The flexural capacity of an FRP reinforced flexural member is dependent on whether the failure is governed by concrete crushing or FRP rupture. The failure mode can be determined by comparing the FRP reinforcement ratio to the balanced reinforcement ratio (that is, a ratio where concrete crushing and FRP rupture occur simultaneously). Because FRP does not yield, the balanced ratio of FRP reinforcement is computed using its design tensile strength. The FRP reinforcement ratio can be computed from Eq. (1), and the balanced FRP reinforcement ratio can be computed from Eq. (2).

$$\rho_f = \frac{A_f}{bd} \longrightarrow (1)$$

$$\rho_{fb} = 0.85\beta_1 \frac{f'_c}{f_{fu} E_f \epsilon_{cu} + f_{fu}} \frac{E_f \epsilon_{cu}}{f_{fu}} \longrightarrow (2)$$

When $\rho_f > \rho_{fb}$, the failure of the member is initiated by crushing of the concrete, and the stress distribution in the concrete can be approximated with the ACI rectangular stress block. The nominal flexural strength can be determined from Eq. (3).

$$M_n = \rho_f f_f \left(1 - 0.59 \frac{\rho_f f_f}{f'_c} \right) b d^2 \longrightarrow (3)$$

Where

$$f_f = \left(\sqrt{\frac{(E_f \epsilon_{cu})^2}{4} + \frac{0.85\beta_1 f'_c}{\rho_f} E_f \epsilon_{cu}} - 0.5 E_f \epsilon_{cu} \right) \leq f_{fu} \longrightarrow (4)$$

When $\rho_f < \rho_{fb}$, the failure of the member is initiated by rupture of FRP bar. The nominal flexural strength at a section can be computed as shown in Eq. (5).

$$M_n = A_f f_{fu} \left(d - \frac{\beta_1 c_b}{2} \right) \longrightarrow (5)$$

Where

$$c_b = \left(\frac{\epsilon_{cu}}{\epsilon_{cu} + \epsilon_{fu}} \right) d \longrightarrow (6)$$

4.1.1 Strength reduction factor for flexure

The strength reduction factor for flexure can be computed by Eq. (7).

$$\phi = \begin{cases} 0.55 & \text{for } \rho_f \leq \rho_{fb} \\ 0.3 + 0.25 \frac{\rho_f}{\rho_{fb}} & \text{for } \rho_{fb} < \rho_f < 1.4\rho_{fb} \\ 0.65 & \text{for } \rho_f \geq 1.4\rho_{fb} \end{cases} \quad \text{---(7)}$$

Table (13): Balance reinforcement ratio modified according the experimental results.

Group	Beam No.	Reinforcement type	b (cm)	d (cm)	Ar (cm ²)	fc (Kg/cm ²)	ρf	ρfb	Failure govern by	ρfb modified	Failure govern by	Mode of Failure
Group D	Dg12	GFRP	12	30	2Ø13	400	0.0084	0.0095	FRP rupture	0.0052	concrete crushing	Flexural-Comp.
	Dc12	CFRP	12	30	2Ø13	400	0.0084	0.0023	concrete crushing	0.0023	concrete crushing	Shear-Comp.
	Ds12	Steel	12	30	2Ø12	400	0.0074	0.0051	concrete crushing	0.0051	concrete crushing	Flexural-Comp.
Group E	Eg12	GFRP	12	30	2Ø13	650	0.0084	0.015	FRP rupture	0.0084	concrete crushing	Flexural-Comp.
	Ec12	CFRP	12	30	2Ø13	650	0.0084	0.0038	concrete crushing	0.0038	concrete crushing	Shear-Comp.
	Es12	Steel	12	30	2Ø12	650	0.0074	0.0051	concrete crushing	0.0051	concrete crushing	Flexural-Comp.
Group A	Ag10	GFRP	12	30	2Ø9	900	0.0046	0.0158	FRP rupture	0.0158	FRP rupture	Flexural
	Ac10	CFRP	12	30	2Ø9	900	0.0046	0.0046	concrete crushing	0.0046	concrete crushing	Shear-Comp.
	As10	Steel	12	30	2Ø10	900	0.0051	0.0051	concrete crushing	0.0051	concrete crushing	Flexural
Group B	Bg12	GFRP	12	30	2Ø13	900	0.0084	0.021	FRP rupture	0.021	FRP rupture	Flexural-Comp.
	Bc12	CFRP	12	30	2Ø13	900	0.0084	0.0052	concrete crushing	0.0084	concrete crushing	Shear-Comp.
	Bs12	Steel	12	30	2Ø12	900	0.0074	0.0051	concrete crushing	0.0051	concrete crushing	Flexural-Comp.
Group C	Cg16	GFRP	12	30	2Ø16	900	0.0132	0.021	FRP rupture	0.01176	concrete crushing	Flexural-Comp.
	Cc(12+12)	CFRP	12	30	4Ø13	900	0.0169	0.0052	concrete crushing	0.0052	concrete crushing	Shear-Comp.
	Cs16	Steel	12	30	2Ø16	900	0.0133	0.0051	concrete crushing	0.0051	concrete crushing	Flexural-Comp.

The failure govern by concrete crushing in the all beams except the beams Ag10 and Bg12 the failure govern by FRP rupture. Because their concrete strength was very high with the small reinforcement ratio. The Eq.(3) and the Eq.(5) used for computing the nominal flexural strength for the beams have the failure govern by concrete crushing and FRP rupture respectively.

Considering the results that come from the experimental works, the presented ρfb by ACI 440 cannot be the exact criteria for detecting the kind of failure, because in a lot of cases where bar ratios were less than the balanced mode, rupture occurred from the compressive area of the concrete. Therefore, regarding the results of experiments, it can be recommended that 0.56 ρfb is to determine the exact criteria of failure. By comparing the ratio of the ultimate moment capacity that comes from the experiments and the nominal moment capacity submitted by ACI 440, it is seen that the said ratio reduced due to a decrease in the bar ratios. This means that with a decrease in the bar ratios, ACI 440 acts more conservative. Regarding ACI 440, this ratio for the mode that is less than the balanced mode is considerably larger than the mode that is more than the balanced mode. Also, an increase in the strength of concrete in most of the cases caused a reduction of this ratio. As it can be seen in Table (13), this ratio for FRP bars is bigger than the steel reference samples. Meanwhile, ACI 440 has been considered a reduction coefficient for nominal moment capacity of sections. As an example, the bar ratio that is less than the balanced mode is 0.5. Including these coefficients in the experiments, it can be said that ACI has been considered as the allowed flexural capacity for the bar ratio that is less than the balanced mode, which is around one fifth of the actual flexural capacity.

The ρfb modified can be computed as shown in Eq. (8).

$$\rho_{fb} = 0.85\beta_1 \frac{f'_c}{f_{fu}E_f\epsilon_{cu} + f_{fu}} \frac{E_f\epsilon_{cu}}{f_{fu}} * 0.56 \quad \text{---(8)}$$

V. Conclusions

This work presents an experimental study on the Behavior of beams reinforced with different types of bars from glass fiber reinforced polymer (GFRP), carbon fiber reinforced polymer (CFRP) and high tensile steel (HTS) under static load, From the test result and their analysis, the following conclusions are obtained

- 1- The beams reinforced by GFRP and CFRP bars behaved linearly up to failure due to the linear characteristics of FRP bars and due to low modulus of elasticity of GFRP and CFRP bars than steel bars. For the beams reinforced by GFRP bars The crack load was appeared after applying 2.00 ton load while in the beams reinforced by CFRP bars and H.T.S it was appear after applying load 3.00 ton. The beams reinforced by H.T.S and CFRP bars had less numbers of cracks than the beams reinforced by GFRP bars at the same applied load specially in the mid of the span. The width of cracks and their extent in the reinforced concrete beams with GFRP in comparison with the reference reinforced by CFRP and H.T.S. The usage of high strength concrete instead of normal concrete creates more cracks, but less width in the reinforced concrete beams with GFRP and CFRP bars.
- 2- The mode of failure for the beams reinforced with GFRP and H.T.S bars were flexural-comp. But in the case of the beams reinforced with CFRP were mainly the failure by the shear – comp. The reinforced concrete beams with GFRP and CFRP bars have an elastic behavior of beams, and after load removal, a major deflection can be seen to go backwards.
- 3- The deflection for the beams reinforced with CFRP bars with the different concrete strength was increased from 1.7 to 2.0 times of the deflection happened in the beam reinforced by H.T.S bars. The deflection was decrease by increase the concrete strength. While the deflection for the beams reinforced with GFRP bars with the different concrete strength was increased from 2.63 to 2.75 times of the deflection happened in the beam reinforced by H.T.S bars. The deflection was slightly decreased by increase the concrete strength. The load-deflection diagram of the reinforced beams with FRP is like a straight line and there is no failure found on it. As such, an increase in concrete strength does not have any effect on deflections when the reinforcement ratio is same in the beams.
- 4- The concrete strain at 85% of ultimate load for the beams reinforced by CFRP ranged from 0.77 to 1.37 the concrete strain at 85% of ultimate load for the beams reinforced by H.T.S bars. While the concrete strain at 85 % of ultimate load for the beams reinforced by GFRP ranged from 1.20 to 1.98 the concrete strain at 85% of ultimate load for the beams reinforced by H.T.S bars.
- 5- The reinforcement strain at 85% of ultimate load for the beams reinforced by CFRP ranged from 0.30 to 0.76 of the reinforcement strain at 85% of ultimate load for the beams reinforced by H.T.S bars. While thereinforcement strainat 85 % of ultimate load for the beams reinforced by GFRP ranged from 0.70 to 2.20 thereinforcement strain at 85% of ultimate load for the beams reinforced by H.T.S bars.
- 6- The slip in the main bar for the beams reinforced by GFRP bars was greater than the slip in the main bar for the beam reinforced by GFRP and H.T.S respectively.
- 7- The reinforcement strain curve for the beam reinforced by GFRP and CFRP was near to the theoretical curves.
- 8- The theoretical Eq. for estimate the nominal flexural strength was given more factor of safety .It ranged from 1.87 to 2.83 times of the theoretical ultimate load for the beams reinforced with CFRP bars and ranged from 5.00 to 6.60 times of the theoretical ultimate load for the beams reinforced by GFRP bars.
- 9- The presented bar ratio ρ_b by ACI 440 is not the exact criterion to recognize the type of failure. Therefore, according to the tests results, 0.56 ρ_{fb} is a more accurate criterion to determine the type of failure that is also according to Chitsazan et al. research result.

$$\rho_{fb} = 0.85\beta_1 \frac{f'_c}{f_{fu}} \frac{E_f \epsilon_{cu}}{E_f \epsilon_{cu} + f_{fu}} * 0.56$$

And also the strength reduction factor for flexural ϕ was range from 0.55 to 0.65 as theoretical but in the actual it was more than that values.it could be increase until 0.80 to be near to the experimental values by reasonable factor of safety.

- 10- The ultimate load for the beams reinforced by CFRP bars ranged from 1.4 to 1.6 of the ultimate load for the beams reinforced by H.T.S bars. And this ratio it was increased until 2.4 for the beams with reinforcement ratio $\mu=0.4\%$.
- 11- The ultimate load for the beams reinforced by GFRP bars was range from 1.1 to 1.15 of the ultimate load for the beams reinforced by H.T.S bars.

12- The Beams reinforced by GFRP and CFRP bars observed that the ultimate loading capacity is more than the beams reinforced by H.T.S bars. And also the stiffness of the beams increased by increasing the concrete strength.

13- When $\rho_f < \rho_{fb}$, the failure of the member is initiated by rupture of FRP bar .The Nominal flexural strength at a section can be computed by

$$M_n = A_f f_{fu} \left(d - \frac{B_1 c_b}{2} \right)$$

So by increasing the reinforcement ratio the ultimate load will increase but by increasing the concrete strength there is small increasing around 5% in ultimate load for the beam had strength C400, C650 and C900 kg/cm².

14-The failure in the beams reinforced by CFRP bar happened in the shear because tensile strength for the CFRP bars is very high almost 5 times of the tensile strength of the steel bars so the failure cannot happened in the flexural if there is no additional reinforcement to resist the shear force.

References

- [1]. ACI Committee 318, 2005, "Building Code Requirements for Structural Concrete (ACI 318-05) and Commentary (318R-05)," American Concrete Institute, Farmington Hills, Mich., 430 pp.
- [2]. ACI Committee 440 (2006). Guide for the Design and Construction of Concrete Reinforced with FRP Bars (ACI 440.1R-06). Am. Concrete Institute, Farmington Hills, Mich., p. 41.
- [3]. Adimi, R.; Rahman, H.; Benmokrane, B.; and Kobayashi, K., 1998, "Effect of Temperature and Loading Frequency on the Fatigue Life of a CFRP Bar in Concrete," Proceedings of the Second International Conference on Composites in Infrastructure (ICCI-98), Tucson, Ariz., V. 2, pp. 203-210.
- [4]. Alsayed SH (1998). Flexural behaviour of concrete beams reinforced with GFRP bars. Cem. Concr. Compos., 20: 1–11.
- [5]. Alsayed SH, Al-Salloum YA, AlMusallam TH (1997). Shear design for beams reinforced by GFRP bars. In: Proceedings of the third int. symposium on non-metallic (FRP) reinforcement for concrete structures (FRPRCS-3), Japan., 2: 285–92.
- [6]. Al-Dulaijan, S. U.; Nanni, A.; Al-Zahrani, M. M.; and Bakis, C. E., 1996, "Bond Evaluation of Environmentally Conditioned GFRP/Concrete System," Proceedings of the Second International Conference on Advanced Composite Materials in Bridges and Structures (ACMBS-2), M. M. El-Badry, ed., Canadian Society for Civil Engineering, Montreal, Quebec, pp. 845-852.
- [7]. Almusallam, T. H.; Al-Salloum, Y.; Alsayed, S.; and Amjad, M., 1997, "Behavior of Concrete Beams Doubly Reinforced by FRP Bars," Proceedings of the Third International Symposium on Non-Metallic (FRP) Reinforcement for Concrete Structures (FRPRCS-3), Japan Concrete Institute, Tokyo, Japan, V. 2, pp. 471-478.
- [8]. Benmokrane, B., 1997, "Bond Strength of FRP Rebar Splices," Proceedings of the Third International Symposium on Non-Metallic (FRP) Reinforcement for Concrete Structures (FRPRCS-3), V. 2, Japan Concrete Institute, Tokyo, Japan, pp. 405-412.
- [9]. Benmokrane, B.; Chaallal, O.; and Masmoudi, R., 1996, "Flexural Response of Concrete Beams Reinforced with FRP Reinforcing Bars," ACI Structural Journal, V. 93, No. 1, Jan.-Feb., pp. 46-55.
- [10]. Benmokrane, B.; El-Salakawy, E.; El-Ragaby, A.; Desgagne, G.; and Lackey, T., 2004, "Design, Construction and Monitoring of Four Innovative Concrete Bridge Decks Using Non-Corrosive FRP Composite Bars," 2004 Annual Conference of the Transportation Association of Canada, Québec City, Québec, Canada.
- [11]. Benmokrane, B., and Rahman, H., eds., 1998, "Durability of Fiber Reinforced Polymer (FRP) Composites for Construction," Proceedings of the First International Conference (CDCC '98), Québec, Canada, 692 pp. Bischoff, P., 2005, "Reevaluation of Deflection Prediction for Concrete Beams Reinforced with Steel and Fiber-Reinforced Polymer Bars," Journal of Structural Engineering, ASCE, V. 131, No. 5, May, pp. 752-767.
- [12]. Brown, V., 1997, "Sustained Load Deflections in GFRP Reinforced Concrete Beams," Proceedings of the Third International Symposium on Non-Metallic (FRP) Reinforcement for Concrete Structures (FRPRCS-3), V. 2, Japan Concrete Institute, Tokyo, Japan, pp. 495-502.
- [13]. Brown, V., and Bartholomew, C., 1996, "Long-Term Deflections of GFRP-Reinforced Concrete Beams," Proceedings of the First International Conference on Composites in Infrastructure (ICCI-96), H. Saadatmanesh and M. R. Ehsani, eds., Tucson, Ariz., pp. 389-400.
- [14]. CAN/CSA-S6-02, 2002, "Design and Construction of Building Components with Fibre-Reinforced Polymers," CAN/CSA S806-02, Canadian Standards Association, Rexdale, Ontario, Canada, 177 pp.
- [15]. Ehsani, M. R., 1993, "Glass-Fiber Reinforcing Bars," Alternative Materials for the Reinforcement and Prestressing of Concrete, J. L. Clarke, Blackie Academic & Professional, London, pp. 35-54.
- [16]. Ehsani, M. R.; Saadatmanesh, H.; and Tao, S., 1995, "Bond of Hooked Glass Fiber Reinforced Plastic (GFRP) Reinforcing Bars to Concrete," ACI Materials Journal, V. 92, No. 4, July-Aug., pp. 391-400.
- [17]. Ehsani, M. R.; Saadatmanesh, H.; and Tao, S., 1996a, "Design Recommendation for Bond of GFRP Rebars to Concrete," Journal of Structural Engineering, V. 122, No. 3, pp. 247-257.
- [18]. Ehsani, M. R.; Saadatmanesh, H.; and Tao, S., 1996b, "Bond Behavior and Design Recommendations for Fiber-Glass Reinforcing Bars," Proceedings of the First International Conference on Composites in Infrastructure (ICCI-96), H. Saadatmanesh and M. R. Ehsani, eds., Tucson, Ariz., pp. 466-476.
- [19]. Faza, S. S., and GangaRao, H. V. S., 1990, "Bending and Bond Behavior of Concrete Beams Reinforced with Plastic Rebars," Transportation Research Record 1290, pp. 185-193.
- [20]. Fiber-Reinforced-Plastic Reinforcement for Concrete Structures—International Symposium, SP-138, A. Nanni and C.W. Dolan, eds., American Concrete Institute, Farmington Hills, Mich., pp. 599-614.
- [21]. Faza, S. S., and GangaRao, H. V. S., 1993b, "Glass FRP Reinforcing Bars for Concrete," Fiber-Reinforced-Plastic (FRP) Reinforcement for Concrete Structures: Properties and Applications, Developments in Civil Engineering, V. 42, A. Nanni, ed., Elsevier, Amsterdam, pp. 167-188.
- [22]. Faza SS, GangaRao HVS (1993). Glass FRP Reinforcing Bars for Concrete. Elsevier Science Publishers B. V. All right reserved, pp. 167-188.
- [23].

- [24]. Grace NF, Soliman AK, Abdel-Sayed G, Saleh KR (1998). Behavior and ductility of simple and continuous FRP reinforced beams. *J. Compos. Constr.*, 2: 186–194.
- [25]. Iman Chitsan et al. (An experimental study on the flexural behavior of FRPRC beams and a comparison of the ultimate moment capacity with ACI), *Journal of Civil Engineering and Construction Technology*, Vol.1 (2), pp.27–42, December 2010, Available online at <http://www.academicjournals.org/icect>.
- [26]. International Federation for Structural Concrete Task Group 9.3 (FRP reinforcement in RC structures) September 2007. <http://fib.epfl.ch> (January 5, 2011).
- [27]. I.F.Kara ,A.F.Ashour (Flexural performance of FRP reinforced concrete beams) *Composite Structure* 94 (2012) 1616-1625, <http://doi:10.1016/j.compstruct.2011.12.012>.
- [28]. Masmoudi R, Thériault M, Benmokrane B (1998). Flexural behavior of concrete beams reinforced with deformed fiber reinforced plastic reinforcing rods. *ACI Struct. J.*, 95: 665–676.
- [29]. Michaluk CR, Rizkalla SH, Tadros G, Benmokrane B (1998). Flexural behavior of one-way concrete slabs reinforced by fiber reinforced plastic reinforcements, *ACI Struct. J.*, 95: 353–365
- [30]. Pecce M, Manfredi G, Cosenza E (2000). Experimental response and code models of GFRP RC beams in bending. *J.Compos. Constr.*, 4:182-190.
- [31]. Saadatmanesh H, Ehsani MR (1991). Fiber Composite Bar for Reinforced Concrete Construction. *J. Compos. Mater.* 25: 188-203.
- [32]. Thériault M, Benmokrane B (1998). Effects of FRP reinforcement ratio and concrete strength on flexural behavior of concrete beams. *J.Compos. Constr.*, 2: 7–16.
- [33]. Tureyen AK, Frosch RJ (2002). Shear tests of FRP-reinforced concrete beams without stirrups. *ACI Struct. J.*, 99: 427–434.
- [34]. Victor C, Shuxin W (2002). Flexural Behavior of Glass Fiber-Reinforced Polymer (GFRP) Reinforced Engineered Cementitious Beams. *ACI Struct. J.*, pp. 11-21.
- [35]. Vijay PV, GangaRao HVS (2001). Bending Behavior and Deformability of Glass Fiber-Reinforced Polymer Reinforced Concrete Members. *ACI Struct. J.*, pp. 834-842.
- [36]. Wenjun Qu et, (2009) (Flexural Behavior of Concrete Beams Reinforced with Hybrid, GFRP and Steel Bars) OF the journal of Composites for Construction, VOL. 13 NO.5 October 1, 2009 ASCE , ISSN 1090-0268/2009/5-350-359.
- [37]. Yost JR, Goodspeed CH, Schmeckpeper ER (2001). Flexural performance of concrete beams reinforced with FRP grids. *J. Compos. Constr.*, 5: 18–25.
- [38]. Yost JR, Gross SP, Dinehart DW (2001). Shear strength of normal strength concrete beams reinforced with deformed GFRP bars. *J.Compos. Constr.*, 5: 268–275.
- [39]. Yost JR, Gross SP (2002). Flexural Design Methodology for Concrete Beams Reinforced with Fiber-Reinforced Polymers. *ACI Struct. J.*, pp. 308-316.
- [40]. AbdElkader.Ahmed.Haridy Flexural Behavior of Concrete Beams Reinforced with Basalt Bars Under Static and Repeated Loads. PH.D Thesis Assuit University 2014.
- [41]. Zakaria Hameed Awadallah Ibrahim Shear Behavior of Concrete Beams Reinforced with Basalt Fiber Reinforced Polymer Rebars. PH.D Thesis Assuit University 2015.